Article

Integration of JAK/STAT receptor-ligand trafficking, signalling and gene expression in Drosophila melanogaster cells

Moore, Rachel, Vogt, Katja, Acosta Martin, Adelina E., Shire, Patrick, Zeidler, Martin and Smythe, Elizabeth

Moore, Rachel, Vogt, Katja ORCID: 0000-0002-4938-563X, Acosta Martin, Adelina E., Shire, Patrick, Zeidler, Martin and Smythe, Elizabeth (2020) Integration of JAK/STAT receptor-ligand trafficking, signalling and gene expression in Drosophila melanogaster cells. Journal of Cell Science, 133 (19). ISSN 0021-9533

Integration of JAK/STAT receptor-ligand trafficking, signalling and gene expression in *Drosophila melanogaster* cells

Rachel Moore[1,], Katja Vogt[1,2], Adelina E. Acosta Martin[3], Patrick Shire[1], Martin Zeidler[1] and Elizabeth Smythe[1]

[1,] Centre for Membrane Interactions and Dynamics
Department of Biomedical Science
University of Sheffield
Sheffield
S10 2TN

Current address
[2,] School of Medicine,
University of Central Lancaster,
Preston
PR1 2HE

[3,] biOMICS Facility
Faculty of Science Mass Spectrometry Centre
University of Sheffield
Sheffield
S10 2TN

Correspondence to: e.smythe@sheffield.ac.uk

Running title: Compartmentalised signalling regulates expression of JAK/STAT targets

Abstract

The JAK/STAT pathway is an essential signalling cascade required for multiple processes during development and for adult homeostasis. A key question in understanding this pathway is how it is regulated in different cell contexts. Here we have examined how endocytic processing contributes to signalling by the single cytokine receptor, Domeless, in *Drosophila melanogaster* cells. We identify an evolutionarily conserved di-Leu motif that is required for Domeless internalisation and show that endocytosis is required for activation of a subset of Domeless targets. Our data indicate that endocytosis both qualitatively and quantitatively regulates Domeless signalling. STAT92E, the single STAT transcription factor in *Drosophila*, appears to be the target of endocytic regulation and our studies show that phosphorylation of STAT92E on Tyr704, while necessary, is not always sufficient for target transcription. Finally, we identify a conserved residue, Thr702, which is essential for Tyr704 phosphorylation. Taken together, our findings identify previously unknown aspects of JAK/STAT pathway regulation likely to play key roles in the spatial and temporal regulation of signalling *in vivo*.

Introduction

The Janus Kinase/Signal transducer and activator of transcription (JAK/STAT) signalling pathway regulates a variety of cellular events, including proliferation and apoptosis, throughout development and in adult life (Villarino et al., 2017). According to the canonical model, JAK/STAT signalling involves the activation of homo- or hetero-dimerised cell-surface transmembrane receptors by ligands, including cytokines, growth factors and hormones, which causes a conformational change in the cytoplasmic tail of the receptor. This stimulates activation of the Janus kinases (JAKs) that are constitutively associated with the receptor. JAK activation leads to specific Tyr phosphorylation of both the kinase and the receptor, subsequently allowing recruitment of signal transducer and activator of transcription (STAT) transcription factors through Src-homology 2 (SH2) domains. This association in turn allows JAK to phosphorylate STATs at a highly conserved C-terminal Tyr residue, leading to STAT dimerization and translocation to the nucleus. Here STATs bind to palindromic DNA sequences to alter expression of target genes, resulting in developmental, haematological and immune-related responses (O'Shea et al., 2015; Stark and Darnell, 2012). Dysregulation of the JAK/STAT pathway is involved in the pathogenesis of diseases such as gigantism, asthma, myocardial hypertrophy, myeloproliferative neoplasia and severe combined immunodeficiency (O'Shea et al., 2015).

The JAK/STAT pathway has been highly conserved through evolution, with invertebrates such as *Drosophila melanogaster* having a full complement of pathway components. However, while mammals have multiple copies of receptors, JAKs and STATs, in *Drosophila* the signalling pathway is composed of a single positively acting receptor, Domeless (Dome) (Brown et al., 2001), a negatively acting receptor, Latran (Makki et al., 2010), one JAK, Hopscotch (Hop), and one STAT, STAT92E (Hou et al., 1996; Yan et al., 1996; Zeidler and Bausek, 2013). Therefore, *Drosophila* provides an excellent model in which to investigate JAK/STAT pathway regulation, without the difficulties of compensation and signalling crosstalk inherent in mammalian systems. In fact, investigating JAK/STAT signalling in *Drosophila* has led to key breakthroughs in understanding the impact of its dysregulation in human disease (Ekas et al., 2010).

The repeated use of the JAK/STAT pathway in a variety of contexts begs the question as to how transcriptional outputs are differentially regulated in a cell- and tissue-specific manner. One potential mechanism to explain this diversity of outputs is regulation by endocytosis (Sigismund and Scita, 2018; Villasenor et al., 2016;

Weinberg and Puthenveedu, 2019). Activated receptors can be internalised into cells by multiple endocytic pathways of which clathrin mediated endocytosis (CME) is the best characterised. Receptor complexes internalised by CME are clustered into clathrin coated pits. The assembled clathrin lattice is linked to the cytoplasmic domains of transmembrane receptors via adaptor proteins, including the AP2 adaptor complex (Mettlen et al., 2018; Owen et al., 2004). In addition to CME, several clathrin independent (CIE) pathways exist which are important for the uptake of particular cargoes (Mayor et al., 2014). Following internalisation, activated receptors are delivered to the early endosome where they may be recycled or targeted to late endosomes and lysosomes for degradation. The Endosomal Sorting Complexes Required for Transport (ESCRT) protein complexes are key for sorting receptors into late endosomes and lysosomes. Hrs is a component of ESCRT-0, acting as an adaptor to select ubiquitinated cargo for targetting to lysosomes. TSG101 is a component of ESCRT I complexes which recruit other ESCRT complexes, which are key in allowing the inward invaginations of the late endosome to form intraluminal vesicles (Henne et al., 2013). Results from *in vivo* and *in vitro* experiments indicate that endocytosis can regulate receptor signalling quantitatively through removal of activated receptors from the cell surface and targeting them to lysosomes for degradation. Endocytosis can also qualitatively regulate signalling by establishing 'signalosomes', which are membrane microdomains within endosomal compartments that allow the recruitment of specific scaffolds, adaptors, kinases and phosphatases, thus resulting in different downstream signalling outputs (Carroll and Dunlop, 2017; Lawrence et al., 2019; Moore et al., 2018; Sigismund and Scita, 2018; Villasenor et al., 2016). The route of entry of activated receptors (CME versus CIE) can also influence signaling output as demonstrated for Notch signaling in *Drosophila* (Shimizu et al., 2014) and TGF-beta signaling in mammalian cells (Di Guglielmo et al., 2003). CME is a major entry portal which has been shown to regulate JAK/STAT signalling following activation of several different cytokine receptors in mammalian cells (Cendrowski et al., 2016; Chmiest et al., 2016; German et al., 2011; Kermorgant and Parker, 2008; Marchetti et al., 2006).

In vivo studies in *Drosophila* suggested that Dome-dependent border cell migration requires ligand-dependent CME and delivery to multivesicular bodies (Devergne et al., 2007). Mutation of endocytic components including clathrin heavy chain (CHC), prevented Dome internalisation, decreased STAT92E expression and nuclear translocation in follicle cells. In contrast, endocytosis appeared to negatively regulate JAK/STAT signalling in *Drosophila* Kc_{167} cells (Müller et al., 2008; Vidal et al., 2010).

These varying results likely reflect differences due to cell context as has been observed for endocytic regulation of receptor tyrosine kinases such as epidermal growth factor receptor (EGFR) (Sousa et al., 2012; Vieira et al., 1996; Villasenor et al., 2015). The underlying regulatory mechanisms of context-dependent signalling are however largely unknown.

Canonical signalling by STAT requires phosphorylation at a conserved Tyr (704 in *Drosophila* STAT92E, isoform C used in this study), which allows for parallel dimerization of STATs via their SH2 domains and translocation into the nucleus. There is also evidence that other posttranslational modifications, in addition to phosphorylation of the conserved Tyr, regulate STAT activity (Chung et al., 1997; Costa-Pereira et al., 2011; Gronholm et al. 2010; Karsten et al., 2006; Wang et al., 2005).

Here we show that in *Drosophila* S2R+ cells, endocytosis is essential for the expression of some, but not all, JAK/STAT pathway target genes. We demonstrate that STAT92E is the target for endocytic regulation and, importantly, that endocytosis qualitatively regulates STAT92E activity. In addition, we have identified a novel phosphorylation site Thr702, which is crucial for Tyr704 phosphorylation of STAT92E.

Results

Dome internalisation requires an evolutionarily conserved di-Leu cassette

To understand mechanisms of Dome internalisation, we first asked how Dome and its ligand Upd2 are taken into cells. Similar to mammalian cells, *Drosophila* cells can internalise material by a variety of CME and CIE mechanisms (Shimizu et al., 2014). It has been shown that Dome is internalised into *Drosophila* Kc_{167} cells by CME (Müller et al., 2008; Vidal et al., 2010). To investigate if this is the case in S2R+ cells, we measured internalisation of Upd2-GFP, as a proxy for receptor internalisation, using an anti-GFP ELISA assay (Wright et al., 2011). We first treated cells with dsRNA targeting Dome and found that there is a significant reduction in the rate (-38%) and extent (-50%) of uptake of Upd2-GFP at both high (20 nM, Figure 1A) and low (3 nM, Fig. S1A) concentrations of Upd2-GFP. Under these conditions levels of Dome mRNA are reduced by ~90% (Figure S1B). The residual uptake of Upd2-GFP in the absence of Dome is likely due to non-specific fluid phase uptake of ligand. When cells were incubated with 20nM Upd2-GFP, knockdown of CHC and AP2 reduced the uptake of Upd2-GFP by approximately 60% compared to knockdown of Dome alone (Figure 1A). Since levels of CHC and AP2 mRNA were reduced by ~80% following dsRNA knockdown, this suggests that the Upd-2-GFP complex can be internalised by CIE as well as CME, as has been shown for several receptors in mammalian cells (Sigismund et al., 2005; Vander Ark et al., 2018) and for Notch and Delta in *Drosophila* (Shimizu et al., 2014). By contrast, when S2R+ cells were incubated with low concentrations of Upd2-GFP (3 nM), knockdown of CHC reduced the uptake of Upd2-GFP to the level observed following Dome knockdown (Figure S1A). Together this suggests that at low concentrations of Upd2-GFP, Dome is primarily internalised by CME, but that increasing concentrations of ligand results in Dome also being internalised via CIE.

Sorting of cargo into clathrin coated pits requires internalisation motifs in the cytoplasmic tails of receptors that include both Tyr- and di-Leu-based motifs (Traub, 2003). Dome is most similar in sequence and structure to gp130, which is a co-receptor shared by receptors for IL-6 (Figure 1B). Internalisation of gp130 requires a di-Leu motif (^{786}LL^{787}) in its cytoplasmic domain (Dittrich et al., 1996) while an upstream serine within the sequence ^{780}**S**ESTQP**LL**^{787} has also been shown to be important for rapid internalisation (Dittrich et al., 1996). Strikingly, the cytoplasmic tail of Dome also contains a di-Leu motif, ^{985}LL^{986}, in a similar context to that of the di-Leu motif in gp130 (Figure 1C). In order to test the potential significance of this motif, we generated a series of FLAG-tagged Dome mutant constructs where individual

elements of the di-Leu cassette were mutated either alone or in combination (Figure 1C), and transfected these constructs into S2R+ cells. To quantitatively measure ligand dependent uptake of the engineered Dome constructs, proteins on the surface of transfected S2R+ cells were biotinylated prior to addition of Upd2-GFP. This showed that while expression of the mutants was somewhat more efficient than transfection of wild-type Dome (Figure S1C), plasma membrane expression all of the constructs was comparable (Figure S1D). Following ligand internalisation, cell surface biotin was removed by treatment with the reducing agent, 2-mercaptoethanesulfonic acid sodium salt, MESNa, while internalised cell surface proteins were protected and remained biotinylated. This allowed the amount of internalised wild-type and mutant Dome to be quantitated. As has been demonstrated previously for Dome (Ren et al., 2015), we observed ligand-independent internalisation of Dome (Figure S1E). We found that mutation of the entire di-Leu cassette to AAASKAA (defined from now on as Dome^{allA}) inhibited internalisation of Dome. Mutation of the di-Leu motif alone (Dome^{LL985AA}-FLAG) did not significantly reduce internalisation. Using site-directed mutagenesis in which we progressively replaced elements of the putative cassette, we established that Glu980 and LL985-6 together represent essential residues required for Dome internalisation (Figure 1D and E). Mutation of Glu980 alone did not significantly affect Dome internalisation (Figure S1F and S1G). Although uptake of Dome $^{E980G/LL985AA}$-FLAG was significantly inhibited (~66%), the effect on internalisation was less than that observed for the Dome^{allA}-FLAG mutant, suggesting that other determinants may also be present within the sequence which are important for Dome internalisation (Figure 1D and 1E). Together these results identify a di-Leu-containing cassette as being essential for Dome internalisation.

Dome signalling is regulated by endocytosis

Dome signalling is known to be regulated by endocytosis in Kc_{167} cells (Müller et al., 2008; Vidal et al., 2010) and *in vivo* (Devergne et al., 2007). To test whether it is similarly regulated in S2R+ cells, we measured the expression of the exogenous reporter *10XSTAT-Luciferase,* which expresses the firefly luciferase enzyme under the control of a minimal promoter downstream of ten STAT92E binding sites (Baeg et al., 2005). As expected, this reporter is activated in S2R+ cells by exogenous Upd2-GFP, in a dose dependent manner (Figure 2A), indicating that these cells express the JAK/STAT pathway components required for activation. We next measured Upd2-GFP-dependent *10xSTAT-Luciferase* reporter activity in control cells and those expressing Dome ^{wt}-FLAG or Dome^{allA}-FLAG (Figure 2B). While expression of

Dome^{wt}-FLAG did not significantly affect signalling, expression of Dome^{allA}-FLAG had a strong dominant negative effect on Upd2-GFP mediated pathway stimulation. This effect was comparable to the level observed in cells expressing Dome$^{Y966A/Q969A}$-FLAG and Dome^{P925I}-FLAG, mutants which have been previously reported to have reduced signalling because of their inability to bind STAT92E (Stahl and Yancopoulos, 1994) and Hop respectively (Fisher et al., 2016). Levels of expression of the transfected proteins are shown in Figure S2A. Together these data demonstrate that Dome mutants that cannot be internalised, also alter JAK/STAT signalling and are consistent with a model where activation of *10XSTAT-Luciferase* by Upd2-GFP is dependent on Dome internalisation.

Endocytosis generates qualitatively different transcriptional outputs.

To further explore a role for endocytosis in regulating signalling downstream of Dome, we asked whether knocking down components of the endocytic machinery might differentially affect expression of Dome target genes. We therefore examined the expression of the *10xSTAT-Luciferase* reporter and the endogenous target genes *socs36E* and *lama* (Flaherty et al., 2009; Karsten et al., 2002) in cells treated with dsRNA to knock down endocytic components. We targeted AP2, an adaptor whose knockdown is predicted to result in accumulation of receptors at the cell surface (Robinson, 2004), Hrs, an adaptor whose knockdown is likely to result in accumulation of ubiquitinated receptors in early endosomes, and TSG101 which is required for the sorting of receptors into intraluminal vesicles and whose knockdown is likely to lead to an accumulation of receptors on the limiting membrane of late endosomes (Henne et al., 2013). Treating cells with dsRNA to knockdown Dome (levels of Dome mRNA were reduced by ~ 90%, Figure S1B) resulted in almost complete abolition of *10XSTAT-Luciferase* expression, demonstrating that both background, and Upd2-GFP-stimulated, reporter activation are receptor-dependent (Figure 2C). In the absence of exogenous ligand, activation of *10XSTAT-Luciferase* in cells treated with dsRNA targeting AP2, Hrs or TSG101, was however unchanged compared to cells treated with control dsRNA (Figure 2C). We speculate that this ligand-independent activation is due to expression of ligands and growth factors that may cross-talk with the JAK/STAT pathway in S2R+ cells (Cherbas et al., 2011). By contrast knockdown of AP2 significantly reduced ligand dependent *10XSTAT-Luciferase* activation whereas knockdown of Hrs or TSG101 had no effect. This indicates that activation of this reporter requires delivery of activated Dome either to, or beyond, an AP2-positive endocytic compartment but prior to an Hrs-positive endosomal compartment. We also examined an endogenous target of Dome,

socs36E (Stec et al., 2013) and found that, in contrast to *10xSTAT-Luciferase* expression, knockdown of both AP2 and Hrs inhibited *socs36E* mRNA expression while knockdown of TSG101 had no effect (Figure 2D). This indicates that activated Dome must be trafficked to an Hrs-positive compartment, or beyond, to allow downstream pathway activation to trigger *socs36E* transcription. Taken together these results indicate that the location of the activated Upd2/Dome complexes within the endocytic pathway can lead to qualitatively different signalling outputs. It is important to note that not all Dome target genes are regulated by endocytosis. For example, expression of *lama*, a well-characterised target of STAT92E (Flaherty et al., 2009), was unaffected when endocytosis was perturbed, suggesting that expression of this target gene mRNA can be driven by activated Upd2:Dome complexes which are located on the plasma membrane (Figure S2B).

Phosphorylation of STAT92E is necessary, but not sufficient, for transcription of some JAK/STAT targets

Upon ligand activation of Dome, STAT92E is phosphorylated by Hop at a conserved Tyr residue (Y704) (Yan et al., 1996). This residue is conserved across all vertebrate STATs, and its phosphorylation is essential for canonical STAT activity and target expression. We therefore asked whether Tyr704 phosphorylation of STAT92E was sensitive to endocytic regulation. One approach to assaying STAT92E phosphorylation utilizes its change in electrophoretic mobility on SDS-PAGE gels (Shi et al., 2008), caused by changes in charge and conformation that occur following phosphorylation (Mao et al., 2005; Wenta et al., 2008). Using this experimental approach, we observed an Upd2 dose-dependent change in the electrophoretic mobility of STAT92E following ligand stimulation (Figure 3A and B), which was reversed by phosphatase treatment (Figure 3C and D). Strikingly, perturbation of the endocytic pathway, by knockdown of AP2 (Figure 3E and F), or Hrs or TSG101 (Figure S3), did not affect the temporal dynamics of STAT92E phosphorylation, a finding that was also confirmed by mass spectrometry (Figure 3G and Supplemental data 1 and 2, available via ProteomeXchange with identifier PXD020719). These data demonstrate that phosphorylation of Tyr704 on STAT92E is not regulated by endocytosis and that other mechanisms must be responsible for the pathway's sensitivity to endocytic regulation.

STAT92E-GFP nuclear import is not affected by knockdown of endocytic components.

Canonical JAK/STAT pathway signalling requires nuclear import of the STAT92E transcription factor to activate gene expression. We therefore investigated whether knockdown of AP2 impaired translocation of STAT92E into the nucleus. Nuclear accumulation can be visualized in S2R+ cells transfected with STAT92E-GFP. In the absence of ligand there appears to be low levels of STAT92E-GFP in the nucleus. This is consistent with reports that STATs shuttle between the nucleus and cytoplasm in a phosphorylation-independent manner and that unphosphorylated nuclear STATs can perform non-canonical functions (Brown and Zeidler, 2008). The levels of nuclear STAT92E-GFP we observe in the absence of Upd2 is also in keeping with reports of GFP-tagged proteins entering the nucleus independently of a nuclear localisation signal (Seibel et al., 2007). When cells are treated with Upd2-GFP (Figure 4A and B), a maximum accumulation is reached after 30 minutes stimulation. This is comparable to the nuclear accumulation of mammalian STATs (McBride et al., 2000) and the time-point at which STAT92E phosphorylation is maximal (data not shown). Consistent with previous studies (Begitt et al., 2000; Schindler et al., 1992), mutation of STAT92E Tyr704 (Y704F) to prevent phosphorylation, abolished nuclear accumulation (Figure 4C). While knockdown of Dome almost completely abolished nuclear accumulation of STAT92E-GFP, knockdown of either AP2 or Hrs had no significant effect, indicating that endocytic trafficking of Upd2/Dome does not regulate nuclear accumulation of STAT92E (Figure 4D). This demonstrates that the loss of target gene expression following AP2 and Hrs knockdown is not likely to be the result of a defect in the translocation of STAT92E into the nucleus.

Thr702 phosphorylation is essential for STAT92E activity

Given that Y704 phosphorylation is necessary but not sufficient for STAT92E-driven pathway gene expression, we wanted to investigate whether other post-translational modifications of STAT92E might be associated with pathway activation. We expressed STAT92E-GFP in S2R+ cells, stimulated with Upd2-GFP, and subjected samples, isolated using GFP-TRAP beads, to mass spectrometry analysis. In addition to Tyr704, this analysis identified Thr47, Ser227 (Figure 5A, Supplemental data 1, 3 and 4, available via ProteomeXchange with identifier PXD020719) and Thr702 (with lower confidence) on STAT92E as being phosphorylated (Supplemental data 1 and 5, available via ProteomeXchange with identifier PXD020719). We therefore decided to test the potential physiological relevance of these newly identified phosphorylation sites using an S2R+ cell line lacking endogenous STAT92E. We used CRISPr/Cas9 to engineer STAT92E negative S2R+ cells,

328 demonstrating that the cell line no longer had detectable STAT92E by Western
329 blotting (Figure S4A) and T7 endonuclease assay (Figure S4B) and was no longer
330 able to activate *10xSTAT-Luciferase* in response to Upd2-GFP (Figure 5B). As
331 expected, expression of wild type STAT92E was able to rescue both Upd2-GFP-
332 dependent and -independent *10XSTAT-Luciferase* activity (Figure S4C) in these
333 STAT92E negative cells, while ligand dependent *10XSTAT-Luciferase* activity was
334 further enhanced by expression of $STAT92E^{K187R}$, a mutant form of STAT92E which
335 cannot be SUMOylated and which has previously been shown to increase Luciferase
336 activity (Gronholm et al., 2010). Taken together, these results demonstrate the utility
337 of the STAT92E negative S2R+ cells for rescue experiments (Figure S4C).
338
339 We next generated mutant forms of STAT92E lacking both known, and candidate,
340 phosphorylation sites (T47V, S227A, T702V and Y704F), and expressed them in
341 STAT92E negative S2R+ cells and measured their ability to activate *10xSTAT-*
342 *Luciferase*. Following ligand stimulation with 0.75nM Upd2-GFP, $STAT92E^{T47V}$
343 $STAT92E^{S227A}$ and $STAT92E^{WT}$ resulted in comparable levels of *10xSTAT-Luciferase*
344 while $STAT92E^{T702V}$ and $STAT92E^{Y704F}$ showed no activation (Figure 5C). This
345 indicates that phosphorylation of Thr702 as well as Tyr704, but not Thr47 or Ser227,
346 is required for JAK/STAT signalling.
347
348 *Phosphomimetic forms of STAT92E rescue signalling*
349 To further explore the role of Thr702 phosphorylation in STAT92E mediated gene
350 activation, we generated phosphomimetics of Thr702 ($STAT92E^{T702D}$, $STAT92E^{T702E}$)
351 and tested their effects on the *10xSTAT-Luciferase* reporter. Using the STAT92E
352 negative S2R+ cell assays, we first showed that expression of 'loss-of-
353 phosphorylation' mutants $STAT92E^{T702V}$ and $STAT92E^{Y704F}$ did not stimulate reporter
354 activity above background levels (Figure 5D). By contrast, expression of both
355 phosphomimetics $STAT92E^{T702D}$ and $STAT92E^{T702E}$ were sufficient to increase both
356 ligand-dependent and ligand-independent *10xSTAT-Luciferase* expression, with
357 $STAT92E^{T702D}$ more effective in both cases. Taken together, we have thus identified a
358 novel posttranslational modification of STAT92E which is essential to trigger
359 transcriptional activity in this assay.
360
361 *Phosphorylation of Thr702 is required for Tyr704 phosphorylation*
362 We next asked whether Thr702 phosphorylation is required for nuclear translocation
363 of STAT92E and found that Upd2-GFP does not stimulate $STAT92E^{T702V}$
364 translocation into the nucleus (Figure 6A and B). Using mass spectrometry, we found

365 that STAT92E^{T702V} showed a substantial reduction in Tyr704 phosphorylation (Figure
366 6C, Supplemental Data 1 and 6, available via ProteomeXchange with identifier
367 PXD020719). This indicates that phosphorylation of Thr702 is essential for efficient
368 phosphorylation of Tyr704 which, in turn, is essential for the bulk of canonical
369 JAK/STAT gene expression.
370

Discussion

In this work we have explored regulatory mechanisms of JAK/STAT signalling following Upd2-dependent Dome activation in *Drosophila* S2R+ cells. We have identified an evolutionarily conserved internalisation motif in the cytoplasmic tail of Dome. We have demonstrated that internalisation and endocytic trafficking of activated Dome allows for compartmentalised signalling to regulate subsets of *Drosophila* JAK/STAT transcriptional targets, through a mechanism that is independent of Tyr704 phosphorylation of STAT92E. We have also demonstrated that phosphorylation of Thr702 is essential for Tyr704 phosphorylation of STAT92E, its translocation to the nucleus and its activity as a transcription factor.

It has been shown that Dome enters cells by CME *in vivo* in *Drosophila* (Devergne et al., 2007) and *in vitro* in Kc_{167} cells (Müller et al., 2008; Vidal et al., 2010). Our results also support a role for CME in Dome uptake in S2R+ cells since dsRNA mediated knockdown of CHC and AP2 reduce Upd2-GFP internalisation. There are a number of defined motifs that allow the inclusion of transmembrane receptors into clathrin coated pits, through interactions with adaptor molecules such as AP2. A di-Leu motif is one such motif, which is well documented to bind to the α-σ2 hemicomplex of AP2 (Doray et al., 2007; Kelly et al., 2008). In this work we have demonstrated that such a motif is part of a cassette, which is essential for efficient internalisation of Dome. Interestingly, a di-Leu-containing cassette is also required for the internalisation of gp130, the closest vertebrate homologue of Dome and the co-receptor for IL-6R, which is necessary for IL-6R internalisation (Dittrich et al., 1996). Similar to gp130, mutation of the di-Leu motif alone in Dome was insufficient to completely abolish internalisation. In the case of gp130, a Ser upstream of the di-Leu motif was also shown to be involved in rapid internalisation. We found that mutation of the equivalent Ser, in combination with mutation of the di-Leu motif, further reduced Dome internalisation although still not to the same extent as in the $Dome^{allA}$ mutant. An acidic residue (Glu or Asp) at -4 position is commonly found adjacent to di-Leu motifs, and its mutation has previously been shown to drastically decrease binding to the α- σ2 hemicomplex of AP2 (Doray et al., 2007). Mutation of this charged residue alone had no effect on receptor internalisation, while mutation of both the Glu and di-Leu reduced internalisation by approximately 66% compared to $Dome^{wt}$. This suggests that while the Glu and di-Leu are important, other residues may also influence Dome internalisation. It also points to an important evolutionary conservation in mechanisms of Dome internalisation in line with the conservation of JAK/STAT pathway components across species.

Our results support a role for CIE, in addition to CME, in uptake of activated Dome in S2R+ cells. While dsRNA-mediated knockdown of CHC and AP2 inhibits internalisation of Upd2-GFP/Dome, the extent of inhibition depends on the concentration of the Upd2-GFP ligand. At low concentrations (3 nM) of Upd2-GFP, there is an absolute requirement for CHC and AP2, whereas at higher concentrations (20 nM), uptake of Upd2-GFP/Dome in cells treated with dsRNA targeting CHC and AP2 is inhibited by approximately 50% compared to cells treated with dsRNA targeting Dome. This is consistent with studies in *Drosophila* where uptake of Notch and Delta through different endocytic pathways (CME and CIE) leads to delivery to different endosomal compartments and differential signalling and the balance of flux between these pathways allows cells to respond to different environmental conditions (Shimizu et al., 2014). Similarly, in mammalian cells, activated receptor tyrosine kinases such as TGF-beta receptors and EGFR can be taken up by CME and CIE, with CME being favoured at lower ligand concentrations (Di Guglielmo et al., 2003; Sigismund et al., 2005). As with Notch signalling, the route of entry of the receptors can determine signalling outcome and receptor fate (Sigismund et al., 2013; Vander Ark et al., 2018). The concept of endocytosis modulating Dome target gene expression in different cells and tissues is supported by previous *in vitro* and *in vivo* studies (Devergne et al., 2007l; Silver et al., 2005; Vidal et al., 2010). Our experiments, which have focussed on CME of activated Dome, indicate that endocytosis also regulates a subset of Dome signalling in S2R+ cells. Mutation of the internalisation motif not only prevents Dome uptake but also prevents Dome activation of *10XSTAT-Luciferase,* consistent with a role for endocytosis in activation of target genes. It is noteworthy that we observe constitutive internalisation and recycling of Dome in the absence of ligand, as has been observed, in mammalian cells, for other cytokine receptors (Thiel et al., 1998). Regulation of constitutive recycling provides cells with a mechanism to control cell surface levels of receptor, which in turn will impact on the magnitude of signalling (Moore et al., 2018).

Strikingly, we have demonstrated that endocytosis of Dome allows an additional level of regulatory control in that delivery to distinct endosomal populations can further affect signalling outcome. Endocytosis is not required for expression of all genes, e.g. *lama,* which is still expressed even when components of the endocytic machinery are ablated with dsRNA. By contrast, expression of *10XSTAT-Luciferase* requires delivery to, or beyond, an AP2-positive compartment, and expression of *socs36E* only occurs when activated Dome has trafficked through an Hrs-positive

compartment, but before it has reached a TSG101-positive compartment (Figure 6D). Our data thus demonstrate that qualitatively different signalling outputs can occur depending on the location of the activated receptor within the endocytic pathway. This strongly supports the concept that the rate at which receptors, in this case Dome, move through the pathway (endocytic flux) is key for signalling outputs and will have profound effects on downstream cell behaviours. This is consistent with studies on EGFR signalling which imply that receptor signalling can modulate the endocytic machinery to determine the rate of receptor flux (Villasenor et al., 2015). Although mechanistic details for endocytic regulation of signalling are better understood for RTKs and GPCRs, there is a considerable body of emerging evidence to support a role for endocytic regulation of cytokine receptors in mammalian cells (Cendrowski et al., 2016). Our data are thus consistent with a variety of studies in mammalian cells demonstrating an instructive role for endocytosis in JAK/STAT signalling (Cendrowski et al., 2016; Chmiest et al., 2016; German et al., 2011; Kermorgant and Parker, 2008; Marchetti et al., 2006).

In *Drosophila*, STAT92E is the single transcription factor utilised by the JAK/STAT pathway to control expression of many different target genes, which are expressed in a tissue-specific and developmentally-regulated manner. The essential role of Tyr704 phosphorylation in JAK/STAT signalling is well-established (Yan et al., 1996). We eliminated the possibility that endocytosis is required for STAT92E phosphorylation by demonstrating that STAT92E is phosphorylated to the same extent, even when components of the endocytic machinery, such as AP2, are knocked down by dsRNA. More importantly what our data demonstrate is that STAT92E Tyr704 phosphorylation, although necessary, is not sufficient for the expression of all Dome target genes. Our data are consistent with previous studies showing that a mutant form of STAT92E, which cannot be methylated is hyper phosphorylated but has a dominant negative effect on target gene expression (Karsten et al., 2006).

When the endocytic pathway is disrupted, phosphorylated STAT92E can still translocate into the nucleus but it is no longer fully signalling competent. This implies that Dome needs to reach a particular endosomal subcompartment or microdomain in order to allow STAT92E to become transcriptionally competent. Of particular interest is the post-Hrs and pre-TSG101 compartment required for *socs36E* expression (Figure 6D). Hrs is a component of ESCRT-0 complex that recognises ubiquitinated signalling cargo destined to be packaged into inward invaginations of the endosomal membrane to form ILVs and ultimately multivesicular bodies. TSG101

is required for later stages of ILV formation (Vietri et al., 2019). As such both these components are found within the same limiting membrane. It has been proposed that membrane microdomains of defined composition, containing signalling molecules, must be able to form within endosomal membranes to generate local signalling competent (signalosome) domains (Shimizu et al., 2014; Teis et al., 2002). Within these specialised signalosomes, STAT92E is likely either to undergo additional posttranslational modifications or to acquire a chaperone protein that facilitates its ability as a transcription factor for a subset of target genes. Support for a Hrs signalosome comes from studies that demonstrate that the Hrs interacting protein STAM is required for downstream signalling following IL2-R activation (Takeshita et al., 1997; Tognon et al., 2014). In mammals, STAMs are phosphorylated in response to a range of cytokines and growth factors (Pandey et al., 2000). The Hrs/STAM complex remains an interesting link between signalling and endocytosis, as it has been shown to have both positive and negative roles in the regulation of RTK signalling in *Drosophila*, which are dependent on the specific tissue and developmental stage (Chanut-Delalande et al., 2010).

Previous studies in mammalian cells have shown that endosomal location is required for STAT3 activation by activated c-Met which is classed as a weak activator, and it was proposed that by localising STAT3 activation in endosomes, nuclear import is facilitated (Kermorgant and Parker, 2008). Here we show the importance of localisation at different points along the endocytic pathway to nuance Dome signalling to allow different signalling outputs with STAT92E being a target for endocytic regulation.

Mass spectrometry analysis revealed Thr702 as a novel phosphorylation site on STAT92E that is functionally important. Mutation to Val which is structurally similar but cannot be phosphorylated, prevented STAT92E Tyr704 phosphorylation and nuclear translocation, while phosphomimetic forms of Thr702 rescued this phenotype. Alignment (Waterhouse et al., 2018) of STAT92E with the published crystal structure of STAT1 (Chen et al., 1998) suggests that Thr702 and Tyr704 are located in a flexible loop region (Figure 6E). Phosphorylation is likely to have significant effects on the conformation of this region. Intriguingly this Thr is conserved in STAT1 and is a phosphomimetic in STAT5 suggesting that it may play a role in ensuring effective Tyr phosphorylation of STATs across species.

Conclusion

In summary we have shown that endocytosis regulates JAK/STAT signalling in *Drosophila* S2R+ cells resulting in qualitatively different signalling outputs. We therefore suggest that the endocytic flux of activated Dome provides a mechanism by which JAK/STAT can regulate different cellular behaviours depending on cell context. In the course of our studies we have shown that while phosphorylation of Tyr704 on STAT92E is necessary, it is not sufficient for expression of some JAK/STAT target genes. Moreover for some targets, delivery to an endosomal sub-compartment is required in order to make STAT92E transcriptionally competent.

Methods

Cell culture

S2R+ cells were cultured at 25°C in Schneider's Insect Tissue Culture media (Gibco, UK), supplemented with 10% heat inactivated FBS (Sigma, UK.), penicillin (1,000 units/ml) and streptomycin (0.1 mg/ml) (Sigma, UK) and 2 mM L-Glutamate (Gibco, UK). Cells were grown to confluency in T75cm^2 flasks and routinely passaged at a 1:3 dilution every 3-4 days.

Cell Transfection

For expression of STAT92E-GFP or Dome-FLAG, cells were seeded a day prior to transfection. They were transfected at a ratio of 2 µg DNA/1x10^6 cells in a 6 well plate, using Effectene Reagent (Qiagen Ltd, UK) and used 2 days later for experiments.

Upd2-GFP production

Upd2-GFP conditioned media was produced essentially as described (Wright et al., 2011) with the following modifications: S2R+ cells were seeded at 1x10^6 cells per well of a 6-well plate 1 day prior to transfection. pAct-Upd2-GFP (2µg per well) was transfected using Effectene Transfection Reagent (Qiagen Ltd, UK) following the manufacturer's instructions. After 2 days, 3 wells of transfected cells were transferred to a T75 cm^2 flask and incubated for a further 4 days. Cells were centrifuged at 1000 x *g* for 3mins, and media was filtered, aliquoted and snap-frozen in liquid N_2 and stored at -80°C. The concentration of Upd2-GFP was determined using an ELISA for GFP (see below). Mock conditioned media (referred to as mock treatment) was produced by transfecting cells with 2 µg pAc5.1 and processed as above.

dsRNA knockdown

dsRNAs were obtained from the Sheffield RNAi Screening Facility whose dsRNA database is based on the Heidelberg 2 library (Boutros lab), generated with Next-RNAi (Horn et al., 2010). It is the redesigned, non-off target effect library, HD2.0 generated using the software next-RNAi (developed by Thomas Horn). Low complexity regions and sequence motifs that induce off-target effects have been excluded. dsRNA probe sizes vary from 81 to 800bp covering ~14000 protein encoding genes and ~1000 non-coding genes (~98.8% coverage). The dsRNA design covers every isoform of each gene and has been optimised for specificity and avoidance of low complexity regions. The following dsRNA amplicons were used; Alpha-adaptin (BKN20148); CHC (BKN20463); Dome (BKN25660); Hrs (BKN27923); TSG101 (BKN28961). Negative control dsRNA was a mixture of 3 amplicons

targeting *C. elegans* mRNA (BKN70003, BKN70004, BKN70005). Amplification of dsRNA was carried out using MEGAscript® RNAi Kit (Life Technologies #AM1626), and purified via ethanol precipitation with sodium acetate, followed by resuspension in sterile water.

Cells were seeded one day prior to knockdown, and resuspended in serum free media on the day of knockdown. The desired number of cells was added to the wells already containing dsRNA and incubated for 1hr at 25°C (15 µg of dsRNA plus $1x10^6$ cells per well in a 6-well plate). After incubation, an equal volume of fresh media containing 20% FBS was added. Cells were incubated at 25°C for a total of 5 days before subsequent experiments. Transfection with STAT92E-GFP was performed on day 3 of dsRNA treatment.

Generation of CRISPr S2R+ cell lines

sgRNA were designed to target the N-terminal coding region of STAT92E and showed <1% chance of off-target activity (crispr.mit.edu). Sequences were also verified using NCBI blast to eliminate potential off-targets. The NGG sequence was then removed, and a G was added to the 5' end of the sgRNA sequence to allow transcription from the U6 promoter in pAc-sgRNA-Cas9 vector. sgRNA oligos (Table 1) were cloned into the pAc-sgRNA-Cas9 expression vector according to the published protocol (Bassett et al., 2014). S2R+ cells were plated at $5x10^5$cells per well in a 12-well plate and transfected with 1 µg pAc-sgRNA-Cas9 construct using Effectene (Qiagen Ltd, UK). After 3 days, puromycin (5 µg ml^{-1}) selection was performed for 7 days before subsequent analysis (Bassett et al., 2014).

Table 1: SgRNA oligos
sgRNA1.1: TTCGACAACACGCCCATGGTTACC
sgRNA1.1: AACGGTAACCATGGGCGTGTTGTC
sgRNA2.1 TTCGACCATGTACCCGGTAACCAT
sgRNA2.2 AACATGGTTACCGGGTACATGGTC

To detect Cas9 induced mutations within the genomic DNA of S2R+ CRISPR cell lines, a T7 endonuclease assay was carried out to identify mismatched, heteroduplex, DNA. PCR products were first produced by amplifying a ~1 kb region around the Cas9 cut site with a 50 µl PCR reaction according to the following method (Guschin et al., 2010). Following verification of size on agarose gels, PCR products were denatured and annealed to form heteroduplexes in the following reaction: 5-10 µl PCR products, 2 µl NEBuffer 2 made up to 19 µl with nuclease free water. The

reaction was heated at in a 95˚C heat block for 10mins and allowed to cool to room temperature. 1 µl of T7 endonuclease was then added to reactions and incubated at 37˚C for 15 mins. The reaction was stopped by addition of 1.5 µl 0.25 M EDTA before running on an agarose gel.

ELISA assay for GFP

The anti-GFP ELISA was performed essentially as described (Wright et al., 2011). Briefly, 96-well high-binding EIA plate (Costar) was coated with 0.0625 µg ml^{-1} goat anti-GFP antibody (Abnova #PAB10341) in 100mM Sodium Bicarbonate overnight at 4°C. The plate was washed 3x with wash buffer (0.2% (w/v) BSA, 0.5% Triton-X 100 in PBS) and then blocked in the same buffer for 1 h at RT. A serial dilution of recombinant GFP (Cellbiolabs, STA-201), starting at 5 ng ml^{-1}, was plated for reference. Samples were incubated for 3 h at 37°C. After washing, the plate was incubated with rabbit anti-GFP (Abcam, Ab290) at 1:20,000 for 2h at RT. After further washes, the plate was incubated with a secondary HRP-linked anti-rabbit antibody (Santa Cruz, sc-2004) at 1:5000 for 1h at RT. Following washing, 200 µl per well of freshly prepared HRP developing solution (0.012% H_2O_2, 0.4 mg ml^{-1} o-phenylenediamine in HRP assay buffer: 51 mM Na_2HPO_4, 27 mM citric acid, pH 5.0, (filtered)) was added to the plate and colour change was observed. To stop the reaction 50 µl of 2 M H_2SO_4 was added per well and the absorbance read at 492 nm on a BMG Labtech plate reader.

Endocytosis assays using anti-GFP ELISA

Cells were seeded in a 24 well plate ($2x10^5$ cells per well) a day prior to experiment. Media was replaced with conditioned media containing established concentrations of Upd2-GFP and incubated at 25°C for various times. Endocytosis was stopped by placing cells on ice and washing twice with ice-cold PBS. Cell-surface ligand was removed by 2x acid washing with 0.2M glycine, 0.15M NaCl pH 2.5 for 2mins. Cells were then washed again in PBS before lysis in ELISA lysis buffer (PBS containing 1 mM $MgCL_2$, 0.1% (w/v) BSA, 0.5% Triton-X 100 supplemented with cOmplete™, Mini, EDTA-free Protease Inhibitor Cocktail (Roche #11836170001)).

Endocytosis assays using cell surface biotinylation

All reactions were carried out on ice unless specified. Growth media was aspirated from cells which were washed 2x with ice-cold PBS. Cells were incubated for 1 hr on ice with freshly prepared EZ-linkTM Sulfo-NHS-SS-Biotin (Thermo Scientific™) (0.25 mg ml^{-1}) before biotin was quenched by washing twice with PBS containing 100 mM

glycine. Internalisation was allowed to proceed for various times by adding pre-warmed Upd2-GFP and incubating at 25°C. Cells were returned to ice and washed 2x with PBS. Cell surface biotin was cleaved by washing cells 3x for 20 mins with MESNa (100 mM 2-mercaptoethanesulfonate, added fresh for each incubation to 50mM Tris-HCL pH8.6, 100 mM NaCl, 1 mM EDTA, 0.2% (w/v) BSA). Cells were then washed 3x in PBS. Reduced disulphide bonds were alkylated for 10mins with 500 mM Iodoacetamide in PBS, before a final 2x PBS wash. Cells were then lysed for 30 mins and lysates were centrifuged at 13,000 rpm for 10 mins. Streptavidin-agarose (15µl) was washed 3x with lysis buffer and incubated with cell lysate (10-30µg) overnight at 4°C with rotation. Beads were then washed 3x with lysis buffer and boiled for 5mins at 95°C in 20 µl Laemmli SDS-PAGE buffer before SDS-PAGE and Western blotting.

Lysis buffer: 20 mM Tris pH7.5, 150 mM NaCl, 1 mM EDTA, 1 mM EGTA, 1% Triton X-100, 1 mM β-Glycerophosphate, 25 mM Na-Pyrophosphate, 1 mM Na_3VO_4, 1 µg ml^{-1} microcystin, 25mM N-ethylmaleimide supplemented with cOmplete™, Mini, EDTA-free Protease Inhibitor Cocktail (Roche #11836170001).

***10xSTAT-Luciferase* detection**

Cells were seeded in a 12-well plate at $5x10^5$ cells per well a day prior to transfection. Cells were transfected with 0.5 µg *10xSTAT-luciferase* and 0.5 µg pAct-Renilla (internal control for transfection) for 1 day and then transferred to a 96-well plate at $5x10^4$ cells per well. Cells were treated with conditioned media containing Upd2-GFP for 18hrs. Luciferase activity was measured using the Dual-Glo Luciferase Assay System (Promega), following manufacturer's instructions, using a 1:5 dilution of DualGlo-luciferase in distilled water. The Dual-Glo Stop and Go Luciferase Assay reagent (1:5 dilution) was added to the plate at an equal volume to the culture media in the wells, and incubated for at least 10mins. The Luciferase firefly signal was measured using a Thermo Scientific™ Varioskan Flash Luminometer. An equal volume of Dual-Glo Stop & Glo Reagent was then added and incubated for at least a further 10 mins to allow measurement of the Renilla firefly (RL) signal. Luciferase activity is calculated as Firefly luciferase value normalized to the internal transfection control (RL).

Calf intestinal alkaline phosphatase (CIP) treatment

STAT92E was immunoprecipitated from cells lysed in lysis buffer (PBS containing 1 mM $MgCl_2$, 0.1% (w/v) BSA, 0.5% Triton-X 100 supplemented with cOmplete™, Mini,

EDTA-free Protease Inhibitor Cocktail (Roche)). CIP (#M0290S NEB) 1 unit per 1µg protein was incubated for 1 hr at 37°C. Reaction was stopped by addition of sample buffer and boiling at 95°C for 5 mins.

Quantitative PCR

RNA extraction was carried out using TRI reagent (Sigma #T9424) and reverse transcribed using the High Capacity RNA-tocDNA™ Kit (Applied Biosystems #4387406). cDNA was diluted 1:10 and relative mRNA levels of *socs36E, Dome*, *lama, AP2, Hrs* and *TSG101* were quantified using qPCR. This was performed using SYBR Green JumpStart™ Taq ReadyMix™ (Sigma #S4438) and primers, listed in Table 2, on the BioRad CFX96 Real time system, C100 Touch™ thermal cycler or the Applied Biosystem QuantStudio 12K Flex. A standard curve of diluted template was used to interpolate the quantity of target gene in the test samples. Results for each target were normalised to levels of the reference gene, ribosomal protein L32 (Rpl32) mRNA, within each well.

Table 2 Primers for qPCR

Gene	CG number	Forward primer	Reverse primer
Rpl32	CG7939	GACGCTTCAAGGGACAGTATCTG	AAACGCGGTTCTGCATGAG
domeless	CG14226	ACTTTCGGTACTCCATCAGC	TGGACTCCACCTTGATGAG
tsg101	CG9712	GAGGAGACACAAATAACAAAGTACC	TGAGTGTCCATCAACCAAATAC
clathrin heavy chain CHC	CG9012	GTAGTAAAGATGACGCAACCAC	GTTCATGTCAATGATGACCACT
α-adaptin	CG4260	ACCAGCGAAAATTAACAAGC	GAGACGACTTCACACCCTTC
socs36A	CG15154	AGTGCTTTACTGCTGCGACT	TCGTCGAGTATTGCGAAGT
lama	CG10645	TGATATTGCTGCTTTCCTGGAC	TGGTTTGGCGATGGTTTTAT

Site-directed mutagenesis

Site-directed mutagenesis was carried out using the QuikChange Site-Directed Mutagenesis Kit (Agilent Technologies) according to manufacturer's instructions. Sequencing of plasmid DNA was carried out at the University of Sheffield's Core Genomic Facility and results analysed using ApE.

Mass spectrometry methods

A detailed description of mass spectrometry methods (sample preparation, mass spectrometry analysis and data processing) together with mass spectrometry data and annotated relevant spectra (phosphorylated Y704, T47, S227, and T702) has been deposited to the ProteomeXchange Consortium via the PRIDE partner repository (Deutsch et al., 2020). The identifier number of the dataset is PXD020719.

Immunofluorescence detection of nuclear and cytoplasmic STAT92E-GFP

A DeltaVision/GE Healthcare OMX optical microscope (version 4) with oil-immersion objective (60x NA 1.42, PlanApochromat Olympus) was used for widefield and SIM immunofluorescence image acquisition. Deconvolution and image registration (for alignment of SIM images) was carried out using the DeltaVision OMX softWoRx 6.0 software. Analysis of microscopy images was carried out using ImageJ. Four regions of interest (ROI) of equal size were drawn within each transfected cell: two within the nucleus and two within the cytoplasm. Intensity measures were averaged for the nucleus and divided by the average intensity for the cytoplasm.

Acknowledgements

RM was funded by a University of Sheffield Centre for Membrane Interactions and Dynamics PhD studentship; KV by a CRUK studentship (C12332/A10681); PS by a BBSRC CASE award (BB/M011151/1). We acknowledge Addgene for the STAT92E-GFP construct. Images were collected in the Wolfson Light Microscopy Facility using a Nikon wide-field camera, funded by MRC Shima award (MR/K015753/1). Mass spectrometry was performed in the University of Sheffield, Faculty of Science biOMICs Facility.

Abbreviations:

JAK/STAT: Janus Kinase/Signal transducer and activator of transcription

CME: clathrin-mediated endocytosis

CIE: clathrin independent endocytosis

ESCRT: Endosomal sorting complexes required for transport

Dome: Domeless

EGFR: epidermal growth factor receptor

RL: Renilla Luciferase

FL : 10xSTAT-Luciferase

CIP: Calf intestinal phosphatase

Figure Legends

Figure 1: Uptake of Upd2-GFP into S2R+ cells is Dome-, clathrin-, and AP2 dependent

(A) S2R+ cells were treated for 5 days with control, clathrin (CHC), AP2, or Dome dsRNA. Cells were incubated with 20 nM Upd2-GFP for indicated time points at 25°C. Following acid washes, cell lysates were analysed with an anti-GFP ELISA. Internalised Upd2-GFP is expressed as percentage of the total amount internalised at 30 minutes. Data represent mean +/- s.d. of two independent experiments. Data were fitted using the non-linear least squares fit in Prism.

(B) Schematic of *Drosophila* Dome and the vertebrate gp130/IL6-R complex.

(C) A di-Leu cassette in the cytoplasmic tail of gp130 and Dome, and mutants generated to investigate internalisation motifs. Note Dome^{AAASKAAL} is referred to as Dome^{allA} in the text.

(D) Quantitation of internalisation of Dome-FLAG wild-type and mutants: Percentage of cell-surface receptor that is internalised after 15 mins at 25°C. Background of biotinylated cell surface Dome-FLAG after 0 mins endocytosis and MESNa treatment was subtracted and internalised Dome-FLAG was then calculated as a percentage of total cell surface Dome-FLAG prior to MESNa treatment. Graphs represent mean +/- s.e.m. for at least 3 independent experiments (Dome$^{E980A/LL985AA}$ = 3 repeats, all other mutants ≥ 4 repeats). *: p<0.5; **: p<0.01; ***: p< 0.001

(E) Sample immunoblot of lysates from cells transfected with Dome^{WT}-FLAG, Dome^{allA}-FLAG, Dome^{LL985AA}-FLAG, Dome$^{E980G/LL985AA}$-FLAG, Dome$^{S979A/LL985AA}$-FLAG, or Dome$^{S981A/LL985AA}$-FLAG, for 48 hrs prior to cell surface biotinylation and incubation at 25°C for times indicated +/- Upd2-GFP and +/-MESNa. Western blots were probed with antibodies as indicated.

Figure 2: Endocytosis regulates Dome target gene expression.

(A) Expression of *10xSTAT-Luciferase* reporter is Upd2-GFP dependent. S2R+ cells were transfected with an actin driven Renilla Luciferase (RL) and *10xSTAT-Luciferase* (FL) reporter construct for 6hrs and then treated with varying concentrations of Upd2-GFP for 30mins, followed by incubation for 18hrs in fresh media, before bioluminescence was measured. Graph represents mean +/- s.d. of 2 experiments, each performed in triplicate.

(B) Mutation of Dome internalisation motifs inhibits Upd2-GFP-induced *10xSTAT-Luciferase* reporter activation. S2R+ cells were transfected with pAc- Ren (RL), *10xSTAT-luciferase* (FL) reporter and pAc5.1 (-) and Dome^{WT}-FLAG, Dome^{allA}-FLAG, Dome$^{Y966A/Q969A}$-FLAG or Dome ^{P925I}-FLAG. Cells were stimulated with 0.75 nM Upd2-

GFP for 30 mins, then incubated in fresh media for 18 hrs. Luciferase activity (FL/RL) is presented as a fold change compared to mock treated cells transfected with pAc5.1 (-). Graph represents mean of triplicates +/- s.e.m. for 4 independent experiments. Parametric, unpaired student's t-test was performed, **: p≤0.01, ***: p≤0.001, ns: not significant.

(C) S2R+ cells were transfected with RL and FL for 6hrs prior to treatment with dsRNA targeting Dome, AP2, Hrs or TSG101 or control (non-targeting), and incubated for five days. Cells were treated with Upd2-GFP for 18hrs and then bioluminescence was measured. Luciferase activity (FL/RL) is normalised to control, mock treated, cells. Graph represents mean of triplicates +/- s.e.m. for 4 experiments. Parametric, unpaired student's t-test carried out to compare Upd2-GFP stimulated samples only, with *: p≤0.05, ****: p≤0.0001.

(D) S2R+ cells were treated with dsRNA against AP2, Hrs and TSG101 as well as non-targeting (control) dsRNA for 5 days. Cells were incubated with 3 nM Upd2-GFP for 2.5 hrs prior to RNA extraction. *socs36* mRNA levels were normalised to that of reference gene Rpl32, and presented as fold change compared to mock-treated control samples. Results are expressed as means of triplicates +/- s.e.m. for 3 independent experiments. Parametric, unpaired student's t-test was carried out to compare Upd2-GFP stimulated samples only. **: p≤0.01

Figure 3: Tyr704 phosphorylation of STAT92E is independent of endocytic regulation

(A) Western blot showing that Upd2-GFP causes a concentration dependent bandshift, indicative of phosphorylation, of STAT92E. The positions of the non-phosphorylated and phosphorylated forms are indicated on the blot.

(B) Graph represents quantitation of phosphorylated STAT92E as a function of Upd2-GFP concentration. Phosphorylated STAT92E is expressed a % of total STAT92E.

(C) S2R+ cells were treated with 3 nM Upd2-GFP for 10mins and lysates incubated with anti-STAT92E antibodies. Immunoprecipitated protein was then treated with calf intestinal phosphatase (CIP), and analysed by SDS-PAGE and immunoblotting with anti-STAT92E antibodies. p-STAT92E and STAT92E are indicated by arrows.

(D) Quantitation of p-STAT92E/STAT92E ratio +/- phosphatase treatment

(E) Representative immunoblot of control vs AP2 knockdown S2R+ cells treated with 3 nM Upd2-GFP at 25°C for the indicated times. Cells were treated with targeting dsRNA cells and incubated for 5 days at 25°C. Total protein extract was analysed by SDS-PAGE and immunoblotted with anti-STAT92E antibodies.

(F) Quantification of STAT92E phosphorylation after AP2 knockdown. Phosphorylated STAT92E is expressed as % total STAT92E. Results are expressed as mean +/- s.e.m. from 4 independent experiments. Using student's t-test there are no statistically significant differences between control and AP2 knockdown samples.
(G) Upd2-dependent phosphorylation of Tyr704 is unchanged following dsRNA mediated knockdown of AP2. S2R+ cells treated with control and AP2 dsRNA were transfected with STAT92E-GFP and treated with 3 nM Upd2-GFP for 75 min. Cells were lysed and incubated with GFP-trap beads prior to preparation for mass spectrometry analysis. Histograms present the ratios Mod/Base of the Y704 phosphorylation site from STAT92E-GFP calculated by MaxQuant software in all conditions. Data shown for n=1.

Figure 4: Upd2-dependent nuclear translocation of STAT92E requires Tyr704 phosphorylation but is independent of endocytosis

(A) Representative images of cells treated with control dsRNA or dsRNA targeting Dome, AP2 or Hrs for 5 days and transfected with $STAT92E^{WT}$-GFP (day 3) and treated with 3 nM Upd2-GFP for 0 or 30 mins.
(B) Time-course of nuclear accumulation of STAT92E-GFP following treatment with Upd2-GFP. Nuclear signal was divided by cytoplasmic signal, and expressed as a percentage of nuclear STAT92E-GFP after 30mins. Data are presented as mean +/- s.d. for at least two independent experiments where >15 cells were examined per experiment.
(C) Quantitation of nuclear versus cytoplasmic $STAT92E^{wt}$-GFP and $STAT92E^{Y704F}$-GFP following treatment of cells with Upd2-GFP for the times indicated. Nuclear signal was divided by cytoplasmic signal, and normalised to 0mins in control cells. Data are presented as mean +/- s.e.m. where at least 80 cells were imaged from 3 independent experiments.
(D) Quantitation of nuclear STAT92E-GFP versus cytoplasmic STAT92E-GFP following treatment of cells with control dsRNA or dsRNA targeting Dome, AP2 or Hrs. Nuclear signal was divided by cytoplasmic signal, and normalised to 0 mins control cells. Data are presented as mean +/- s.e.m. for 3 independent experiments where at least 20 cells were imaged per condition per experiment, with parametric, unpaired student's t-test being performed. ****: $p \leq 0.0001$; ns is non significant.

Figure 5: Phosphorylation of Thr702 on STAT92E is essential for its function

(A) Schematic of STAT92E indicating domains, Tyr704 and novel phosphorylation sites that were identified by mass spectrometry.

(B) Control (WT) or cells lines lacking STAT92E (crSTAT) cell lines were transfected with pAc- Ren (RL), *10xSTATluciferase* (FL) reporter and pAc5.1(-) for 24 hrs. Cells were stimulated with 3 nM Upd2-GFP for 30 mins, and then incubated in fresh media for 18 hrs. Luciferase activity (FL/RL) is expressed as a fold change compared to mock treated cells transfected with pAc5.1 (-). Graph represents mean +/- s.e.m. of triplicates from 3 independent experiments. Parametric, unpaired student's t-test was performed with ****: p≤0.0001.

(C) STAT92E mutants which cannot be phosphorylated, $STAT92E^{T702V}$ and $STAT92E^{Y704F}$, inhibit Upd2-GFP-dependent signalling. crSTAT cells were transfected with pAc-Ren, *10xSTAT-Luciferase* and pAc5.1 (-), and/or STAT92E-GFP mutants as indicated. Cells were mock-treated or stimulated with 0.75 nM Upd2-GFP for 30 mins, and then incubated in fresh media for 18 hrs. Data are mean +/- s.e.m. from 3 independent experiments, each performed in triplicate and normalised to cells transfected with pAc5.1 (-). Parametric, unpaired student's t-test was performed with **: p≤0.01, ****: p≤0.0001.

(D) Phosphomimetic forms of STAT92E rescue inhibitory effects of T702V on Upd2-GFP-dependent signalling. crSTAT cells were transfected with pAc-Ren*, 10xSTAT-Luciferase* and pAc5.1 (-) and/or STAT92E-GFP mutants as indicated. Cells were mock-treated or stimulated with 0.75 nM Upd2-GFP for 30 mins, then incubated in fresh media for 18 hrs. Luciferase activity (FL/RL) is expressed as a fold change compared to mock treated cells transfected with pAc5.1 (-). Data is expressed as mean +/- s.e.m. from 3 independent experiments and normalised to mock-treated cells transfected with pAc5.1. Parametric, unpaired student's t-test was performed, with *: p≤0.05, **: p≤0.01, ***: p≤0.001, ns: non significant.

Figure 6: Phosphorylation of Thr702 is essential for Tyr704 phosphorylation

(A) T702V mutation prevents STAT92E-GFP nuclear translocation in response to ligand. Representative images of crSTAT cells transfected with either $STAT92E^{WT}$-GFP or $STAT92E^{T702V}$-GFP, and treated with 3 nM Upd2-GFP for 0, 15 or 30 mins.

(B) Nuclear signal was divided by cytoplasmic signal, and normalised to 0 mins control cells. Data is presented as mean +/-s.e.m. for 3 independent experiments, where at least 30 cells were imaged per condition per experiment. Parametric, unpaired student's t-test being performed. ****: p≤0.0001, ns: non significant

(C) Mutation of Thr702 reduces phosphorylation on Tyr704. S2R+ cells were transfected with $STAT92E^{WT}$-GFP or $STAT92E^{T702V}$-GFP for 2 days prior to treatment with 3nM Upd2-GFP for 75mins. Cells were lysed and incubated with GFP-trap beads prior to preparation for mass spectrometry analysis. Histograms present the

ratios Mod/Base of Y704 phosphorylation site from STAT92E^{WT}-GFP and STAT92E^{T702V}-GFP calculated by MaxQuant software. Data shown for n=1.
(D) Compartmentalised signalling regulates expression of JAK/STAT targets. Cartoon depicting how movement of the Upd2/Dome complex along the endocytic pathway regulates differential gene expression. At the cell surface activated Dome can result in transcription of a subset of target genes (e.g. *lama*, shown in green). Following uncoating of clathrin and AP2 from clathrin coated vesicles, other genes can be activated (e.g. *Luciferase*, shown in orange). Hrs selects ubiquitinated cargo for incorporation into intraluminal vesicles but activated Dome can still signal to activate other genes (e.g. *socs36E*, shown in purple) before TSG101 results in its incorporation into inward invaginations of the endosomal membrane to form intra luminal vesicles which results in termination of signalling.
(E) Thr702 conservation and location within STAT1 crystal structure. (i) Alignment of sequences surrounding the conserved Tyr in STAT92E-C (C isoform), STAT92E-F (long isoform), human STAT1, STAT5a and STAT5b. The conserved Tyr is highlighted in orange, and a conserved Lys highlighted in green. The Thr residue is in a yellow box. ii) Crystal structure of STAT1 (PDB:1bf5). iii) Location of the Thr and Tyr residues within the STAT1 crystal structure.

Supplementary Legends

Figure S1:

(A) CME is the route of GFP-Upd2 uptake at low ligand concentrations. S2R+ cells were treated for 5 days with control, clathrin (CHC) or Dome dsRNA. Cells were incubated with 3 nM Upd2-GFP for indicated time points at 25°C. Following acid washes, cell lysates were analysed with an anti-GFP ELISA. Internalised Upd2-GFP is expressed as percentage of the total amount internalised at 30 minutes. Graph is a representative experiment where each point is mean of triplicates +/- s.d.

(B) mRNA levels of dsRNA targets following knockdown. S2R+ cells were treated with dsRNA 5 days prior to TRIzol RNA extraction. mRNA levels were analysed using qPCR, with levels of target mRNA normalised to rpl32 mRNA. Ratios are plotted as fold change compared to control dsRNA for each target mRNA. Graph represents the mean of triplicates +/- s.d. for at least 2 independent experiments (Dome = 2 repeats), or mean +/- s.e.m. for at least three independent experiments (AP2, Hrs and TSG101). Parametric, unpaired student's t-test was performed to compare control knockdown with targeted dsRNA knockdown, with ***p≤0.001, ****p≤0.0001.

(C) Lysates from S2R+ cells transfected with FLAG-tagged Dome wild-type and mutants were prepared and subjected to SDS-PAGE and Western blotting with antibodies to FLAG and β-actin. The ratio of transfected Dome-FLAG construct is expressed as a function of the amount of β-actin. Graph is the mean ± s.d. of at least 2 independent experiments. Using student's t-test, there was no statistical difference between wild-type and mutant constructs.

(D) Percentage of biotinylated Dome-FLAG at cell surface compared to total levels of transfected Dome-FLAG in cells expressing wild-type or mutant Dome-FLAG constructs. Using student's t-test, there was no statistical difference between wild-type and mutant constructs.

(E) Dome is internalised efficiently in the absence of ligand. Sample immunoblot of cells transfected with $Dome^{WT}$-FLAG for 48hrs prior to cell surface biotinylation and endocytosis for 15 minutes +/- Upd2-GFP, followed by treatment +/- MESNa. Western blots were probed with antibodies as indicated.

(F) Sample immunoblot of lysates from cells transfected with $Dome^{WT}$-FLAG or $Dome^{E980A}$-FLAG for 48 hrs prior to cell surface biotinylation and incubation at 25°C for times indicated +/- Upd2-GFP followed by treatment +/- MESNa. Western blots were probed with antibodies as indicated.

(G) Quantitation of internalisation of Dome^{WT}-FLAG and Dome^{E980A}-FLAG. Percentage of cell-surface receptor that is internalised after 15 mins at 25°C. Background of biotinylated cell surface Dome-FLAG after 0 mins endocytosis and MESNa treatment was subtracted and internalised Dome-FLAG was then calculated as a percentage of total cell surface Dome-FLAG prior to MESNa treatment. Graphs represent mean +/- s.d. for 2 independent experiments and no significant differences were observed.

Figure S2:
(A) Sample immunoblot of relative transfection efficiencies of Dome^{WT}-FLAG, Dome^{allA}-FLAG, Dome$^{Y966A/Q969A}$-FLAG and Dome ^{P925I}-FLAG. Blots were probed with antibodies as indicated.
(B) *lama* expression is independent of endocytosis. S2R+ cells were treated with dsRNA against AP2, Hrs and TSG101 as well as non-targeting (control) dsRNA for 5 days. Cells were incubated with 3 nM Upd2-GFP for 2.5 hrs prior to RNA extraction. *lama* mRNA levels were normalised to that of reference gene Rpl32, and presented as fold change compared to mock-treated control samples. Results are expressed as means of triplicates +/- s.e.m. for 3 independent experiments.

Figure S3: STAT92E phosphorylation is not regulated by endocytosis. Representative immunoblot of control vs AP2, Hrs and TSG101 knockdown S2R+ cells treated with 3 nM Upd2-GFP at 25°C for the indicated times. Cells were treated with targeting dsRNA and incubated for 5 days at 25°C. Total protein extract was analysed by SDS-PAGE and immunoblotted with anti-STAT92E antibodies.

Figure S4: Generation and characterization of STAT92E negative S2R+ cells.
(A) Immunoblot and quantification demonstrating levels of STAT92E protein in cells transfected with pAc-sgRNA-Cas9 targeting STAT92E for 3 days, and then either with or without puromycin selection as indicated. Blots were probed with antibodies as indicated.
(B) T7-endonuclease assay demonstrates Cas9 induced mutation in the STAT92E gene. Genomic DNA was extracted from WT and crSTAT2 cell lines, and a 989bp region around the sgRNA target site was amplified by PCR. Addition of T7 endonuclease to the PCR product causes multiple bands for crSTAT2 cell line but not WT cells.
(C) Mutation of Lys187 increases STAT92E signalling. crSTAT cells were transfected with pAc-Ren, *10xSTAT-Luciferase* and pAc5.1 (-), STAT92E^{WT}-GFP or

974 STAT92E^{K187R}-GFP. Cells were stimulated with 0.75 nM Upd2-GFP for 30 mins, then
975 incubated in fresh media for 18 hrs followed by measurement of bioluminescence.
976 Data is mean +/- s.e.m. from 3 independent experiments and normalised to cells
977 transfected with pAc5.1 (-) and treated with 0 nM Upd2-GFP. *: $p<0.05$; **: $p<0.01$.
978
979

References

Baeg, G. H., Zhou, R. and Perrimon, N. (2005). Genome-wide RNAi analysis of JAK/STAT signaling components in Drosophila. *Genes Dev* **19**, 1861-70.

Bassett, A. R., Tibbit, C., Ponting, C. P. and Liu, J. L. (2014). Mutagenesis and homologous recombination in Drosophila cell lines using CRISPR/Cas9. *Biol Open* **3**, 42-9.

Begitt, A., Meyer, T., van Rossum, M. and Vinkemeier, U. (2000). Nucleocytoplasmic translocation of Stat1 is regulated by a leucine-rich export signal in the coiled-coil domain. *Proc Natl Acad Sci U S A* **97**, 10418-23.

Brown, S., Hu, N. and Hombria, J. C. (2001). Identification of the first invertebrate interleukin JAK/STAT receptor, the Drosophila gene domeless. *Curr Biol* **11**, 1700-5.

Brown, S. and Zeidler, M. P. (2008). Unphosphorylated STATs go nuclear. *Curr Opin Genet Dev* **18**, 455-60.

Carroll, B. and Dunlop, E. A. (2017). The lysosome: a crucial hub for AMPK and mTORC1 signalling. *Biochem J* **474**, 1453-1466.

Cendrowski, J., Maminska, A. and Miaczynska, M. (2016). Endocytic regulation of cytokine receptor signaling. *Cytokine Growth Factor Rev* **32**, 63-73.

Chanut-Delalande, H., Jung, A. C., Baer, M. M., Lin, L., Payre, F. and Affolter, M. (2010). The Hrs/Stam complex acts as a positive and negative regulator of RTK signaling during Drosophila development. *PLoS One* **5**, e10245.

Chen, X., Vinkemeier, U., Zhao, Y., Jeruzalmi, D., Darnell, J. E., Jr. and Kuriyan, J. (1998). Crystal structure of a tyrosine phosphorylated STAT-1 dimer bound to DNA. *Cell* **93**, 827-39.

Cherbas, L., Willingham, A., Zhang, D., Yang, L., Zou, Y., Eads, B. D., Carlson, J. W., Landolin, J. M., Kapranov, P., Dumais, J. et al. (2011). The transcriptional diversity of 25 Drosophila cell lines. *Genome Res* **21**, 301-14.

Chmiest, D., Sharma, N., Zanin, N., Viaris de Lesegno, C., Shafaq-Zadah, M., Sibut, V., Dingli, F., Hupe, P., Wilmes, S., Piehler, J. et al. (2016). Spatiotemporal control of interferon-induced JAK/STAT signalling and gene transcription by the retromer complex. *Nat Commun* **7**, 13476.

Chung, J., Uchida, E., Grammer, T. C. and Blenis, J. (1997). STAT3 serine phosphorylation by ERK-dependent and -independent pathways negatively modulates its tyrosine phosphorylation. *Mol Cell Biol* **17**, 6508-16.

Costa-Pereira, A. P., Bonito, N. A. and Seckl, M. J. (2011). Dysregulation of janus kinases and signal transducers and activators of transcription in cancer. *Am J Cancer Res* **1**, 806-16.

Deutsch, E. W., Bandeira, N., Sharma, V., Perez-Riverol, Y., Carver, J. J., Kundu, D. J., Garcia-Seisdedos, D., Jarnuczak, A. F., Hewapathirana, S., Pullman, B. S. et al. (2020). The ProteomeXchange consortium in 2020: enabling 'big data' approaches in proteomics. *Nucleic Acids Res* **48**, D1145-D1152.

Devergne, O., Ghiglione, C. and Noselli, S. (2007). The endocytic control of JAK/STAT signalling in Drosophila. *J Cell Sci* **120**, 3457-64.

Di Guglielmo, G. M., Le Roy, C., Goodfellow, A. F. and Wrana, J. L. (2003). Distinct endocytic pathways regulate TGF-beta receptor signalling and turnover. *Nat Cell Biol* **5**, 410-21.

Dittrich, E., Haft, C. R., Muys, L., Heinrich, P. C. and Graeve, L. (1996). A di-leucine motif and an upstream serine in the interleukin-6 (IL-6) signal transducer gp130 mediate ligand-induced endocytosis and down-regulation of the IL-6 receptor. *J Biol Chem* **271**, 5487-94.

Doray, B., Lee, I., Knisely, J., Bu, G. and Kornfeld, S. (2007). The gamma/sigma1 and alpha/sigma2 hemicomplexes of clathrin adaptors AP-1 and AP-2 harbor the dileucine recognition site. *Mol Biol Cell* **18**, 1887-96.

Ekas, L. A., Cardozo, T. J., Flaherty, M. S., McMillan, E. A., Gonsalves, F. C. and Bach, E. A. (2010). Characterization of a dominant-active STAT that promotes tumorigenesis in Drosophila. *Dev Biol* **344**, 621-36.

Fisher, K. H., Stec, W., Brown, S. and Zeidler, M. P. (2016). Mechanisms of JAK/STAT pathway negative regulation by the short coreceptor Eye Transformer/Latran. *Mol Biol Cell* **27**, 434-41.

Flaherty, M. S., Zavadil, J., Ekas, L. A. and Bach, E. A. (2009). Genome-wide expression profiling in the Drosophila eye reveals unexpected repression of notch signaling by the JAK/STAT pathway. *Dev Dyn* **238**, 2235-53.

German, C. L., Sauer, B. M. and Howe, C. L. (2011). The STAT3 beacon: IL-6 recurrently activates STAT 3 from endosomal structures. *Exp Cell Res* **317**, 1955-69.

Gronholm, J., Ungureanu, D., Vanhatupa, S., Ramet, M. and Silvennoinen, O. (2010). Sumoylation of Drosophila transcription factor STAT92E. *J Innate Immun* **2**, 618-24.

Guschin, D. Y., Waite, A. J., Katibah, G. E., Miller, J. C., Holmes, M. C. and Rebar, E. J. (2010). A rapid and general assay for monitoring endogenous gene modification. *Methods Mol Biol* **649**, 247-56.

Henne, W. M., Stenmark, H. and Emr, S. D. (2013). Molecular mechanisms of the membrane sculpting ESCRT pathway. *Cold Spring Harb Perspect Biol* **5**.

Horn, T., Sandmann, T. and Boutros, M. (2010). Design and evaluation of genome-wide libraries for RNA interference screens. *Genome Biol* **11**, R61.

Hou, X. S., Melnick, M. B. and Perrimon, N. (1996). Marelle acts downstream of the Drosophila HOP/JAK kinase and encodes a protein similar to the mammalian STATs. *Cell* **84**, 411-9.

Karsten, P., Hader, S. and Zeidler, M. P. (2002). Cloning and expression of Drosophila SOCS36E and its potential regulation by the JAK/STAT pathway. *Mech Dev* **117**, 343-6.

Karsten, P., Plischke, I., Perrimon, N. and Zeidler, M. P. (2006). Mutational analysis reveals separable DNA binding and trans-activation of Drosophila STAT92E. *Cell Signal* **18**, 819-29.

Kelly, B. T., McCoy, A. J., Spate, K., Miller, S. E., Evans, P. R., Honing, S. and Owen, D. J. (2008). A structural explanation for the binding of endocytic dileucine motifs by the AP2 complex. *Nature* **456**, 976-979.

Kermorgant, S. and Parker, P. J. (2008). Receptor trafficking controls weak signal delivery: a strategy used by c-Met for STAT3 nuclear accumulation. *J Cell Biol* **182**, 855-63.

Lawrence, R. E., Fromm, S. A., Fu, Y., Yokom, A. L., Kim, D. J., Thelen, A. M., Young, L. N., Lim, C. Y., Samelson, A. J., Hurley, J. H. et al. (2019). Structural mechanism of a Rag GTPase activation checkpoint by the lysosomal folliculin complex. *Science* **366**, 971-977.

Makki, R., Meister, M., Pennetier, D., Ubeda, J. M., Braun, A., Daburon, V., Krzemien, J., Bourbon, H. M., Zhou, R., Vincent, A. et al. (2010). A short receptor downregulates JAK/STAT signalling to control the Drosophila cellular immune response. *PLoS Biol* **8**, e1000441.

Mao, X., Ren, Z., Parker, G. N., Sondermann, H., Pastorello, M. A., Wang, W., McMurray, J. S., Demeler, B., Darnell, J. E., Jr. and Chen, X. (2005). Structural bases of unphosphorylated STAT1 association and receptor binding. *Mol Cell* **17**, 761-71.

Marchetti, M., Monier, M. N., Fradagrada, A., Mitchell, K., Baychelier, F., Eid, P., Johannes, L. and Lamaze, C. (2006). Stat-mediated signaling induced by type I and type II interferons (IFNs) is differentially controlled through lipid microdomain association and clathrin-dependent endocytosis of IFN receptors. *Mol Biol Cell* **17**, 2896-909.

Mayor, S., Parton, R. G. and Donaldson, J. G. (2014). Clathrin-Independent Pathways of Endocytosis. *Cold Spring Harbor Perspectives in Biology* **6**.

McBride, K. M., McDonald, C. and Reich, N. C. (2000). Nuclear export signal located within theDNA-binding domain of the STAT1transcription factor. *EMBO J* **19**, 6196-206.

Mettlen, M., Chen, P. H., Srinivasan, S., Danuser, G. and Schmid, S. L. (2018). Regulation of Clathrin-Mediated Endocytosis. *Annu Rev Biochem* **87**, 871-896.

Moore, R., Pujol, M. G., Zhu, Z. and Smythe, E. (2018). Interplay of Endocytosis and Growth Factor Receptor Signalling. *Prog Mol Subcell Biol* **57**, 181-202.

Müller, P., Boutros, M. and Zeidler, M. P. (2008). Identification of JAK/STAT pathway regulators--insights from RNAi screens. *Semin Cell Dev Biol* **19**, 360-9.

O'Shea, J. J., Schwartz, D. M., Villarino, A. V., Gadina, M., McInnes, I. B. and Laurence, A. (2015). The JAK-STAT pathway: impact on human disease and therapeutic intervention. *Annu Rev Med* **66**, 311-28.

Owen, D. J., Collins, B. M. and Evans, P. R. (2004). Adaptors for clathrin coats: structure and function. *Annu Rev Cell Dev Biol* **20**, 153-91.

Pandey, A., Fernandez, M. M., Steen, H., Blagoev, B., Nielsen, M. M., Roche, S., Mann, M. and Lodish, H. F. (2000). Identification of a novel immunoreceptor tyrosine-based activation motif-containing molecule, STAM2, by mass spectrometry and its involvement in growth factor and cytokine receptor signaling pathways. *J Biol Chem* **275**, 38633-9.

Ren, W., Zhang, Y., Li, M., Wu, L., Wang, G., Baeg, G. H., You, J., Li, Z. and Lin, X. (2015). Windpipe controls Drosophila intestinal homeostasis by regulating JAK/STAT pathway via promoting receptor endocytosis and lysosomal degradation. *PLoS Genet* **11**, e1005180.

Robinson, M. S. (2004). Adaptable adaptors for coated vesicles. *Trends Cell Biol* **14**, 167-74.

Schindler, C., Shuai, K., Prezioso, V. R. and Darnell, J. E., Jr. (1992). Interferon-dependent tyrosine phosphorylation of a latent cytoplasmic transcription factor. *Science* **257**, 809-13.

Seibel, N. M., Eljouni, J., Nalaskowski, M. M. and Hampe, W. (2007). Nuclear localization of enhanced green fluorescent protein homomultimers. *Anal Biochem* **368**, 95-9.

Shi, S., Larson, K., Guo, D., Lim, S. J., Dutta, P., Yan, S. J. and Li, W. X. (2008). Drosophila STAT is required for directly maintaining HP1 localization and heterochromatin stability. *Nat Cell Biol* **10**, 489-96.

Shimizu, H., Woodcock, S. A., Wilkin, M. B., Trubenova, B., Monk, N. A. and Baron, M. (2014). Compensatory flux changes within an endocytic trafficking network maintain thermal robustness of Notch signaling. *Cell* **157**, 1160-74.

Sigismund, S., Algisi, V., Nappo, G., Conte, A., Pascolutti, R., Cuomo, A., Bonaldi, T., Argenzio, E., Verhoef, L. G., Maspero, E. et al. (2013). Threshold-controlled ubiquitination of the EGFR directs receptor fate. *EMBO J* **32**, 2140-57.

Sigismund, S. and Scita, G. (2018). The 'endocytic matrix reloaded' and its impact on the plasticity of migratory strategies. *Curr Opin Cell Biol* **54**, 9-17.

Sigismund, S., Woelk, T., Puri, C., Maspero, E., Tacchetti, C., Transidico, P., Di Fiore, P. P. and Polo, S. (2005). Clathrin-independent endocytosis of ubiquitinated cargos. *Proc Natl Acad Sci U S A* **102**, 2760-5.

Silver, D. L., Geisbrecht, E. R. and Montell, D. J. (2005). Requirement for JAK/STAT signaling throughout border cell migration in Drosophila. *Development* **132**, 3483-92.

Sousa, L. P., Lax, I., Shen, H., Ferguson, S. M., De Camilli, P. and Schlessinger, J. (2012). Suppression of EGFR endocytosis by dynamin depletion

reveals that EGFR signaling occurs primarily at the plasma membrane. *Proc Natl Acad Sci U S A* **109**, 4419-24.

Stahl, N. and Yancopoulos, G. D. (1994). The tripartite CNTF receptor complex: activation and signaling involves components shared with other cytokines. *J Neurobiol* **25**, 1454-66.

Stark, G. R. and Darnell, J. E., Jr. (2012). The JAK-STAT pathway at twenty. *Immunity* **36**, 503-14.

Stec, W., Vidal, O. and Zeidler, M. P. (2013). Drosophila SOCS36E negatively regulates JAK/STAT pathway signaling via two separable mechanisms. *Mol Biol Cell* **24**, 3000-9.

Takeshita, T., Arita, T., Higuchi, M., Asao, H., Endo, K., Kuroda, H., Tanaka, N., Murata, K., Ishii, N. and Sugamura, K. (1997). STAM, signal transducing adaptor molecule, is associated with Janus kinases and involved in signaling for cell growth and c-myc induction. *Immunity* **6**, 449-57.

Teis, D., Wunderlich, W. and Huber, L. A. (2002). Localization of the MP1-MAPK scaffold complex to endosomes is mediated by p14 and required for signal transduction. *Dev Cell* **3**, 803-14.

Thiel, S., Dahmen, H., Martens, A., Muller-Newen, G., Schaper, F., Heinrich, P. C. and Graeve, L. (1998). Constitutive internalization and association with adaptor protein-2 of the interleukin-6 signal transducer gp130. *FEBS Lett* **441**, 231-4.

Tognon, E., Wollscheid, N., Cortese, K., Tacchetti, C. and Vaccari, T. (2014). ESCRT-0 is not required for ectopic Notch activation and tumor suppression in Drosophila. *PLoS One* **9**, e93987.

Traub, L. M. (2003). Sorting it out: AP-2 and alternate clathrin adaptors in endocytic cargo selection. *J Cell Biol* **163**, 203-8.

Vander Ark, A., Cao, J. and Li, X. (2018). TGF-beta receptors: In and beyond TGF-beta signaling. *Cell Signal* **52**, 112-120.

Vidal, O. M., Stec, W., Bausek, N., Smythe, E. and Zeidler, M. P. (2010). Negative regulation of Drosophila JAK-STAT signalling by endocytic trafficking. *J Cell Sci* **123**, 3457-66.

Vieira, A. V., Lamaze, C. and Schmid, S. L. (1996). Control of egf receptor signaling by clathrin-mediated endocytosis. *Science* *274*, 2086-2089.

Vietri, M., Radulovic, M. and Stenmark, H. (2019). The many functions of ESCRTs. *Nat Rev Mol Cell Biol*.

Villarino, A. V., Kanno, Y. and O'Shea, J. J. (2017). Mechanisms and consequences of Jak-STAT signaling in the immune system. *Nat Immunol* **18**, 374-384.

Villasenor, R., Kalaidzidis, Y. and Zerial, M. (2016). Signal processing by the endosomal system. *Curr Opin Cell Biol* **39**, 53-60.

Villasenor, R., Nonaka, H., Del Conte-Zerial, P., Kalaidzidis, Y. and Zerial, M. (2015). Regulation of EGFR signal transduction by analogue-to-digital conversion in endosomes. *Elife* **4**.

Wang, R., Cherukuri, P. and Luo, J. (2005). Activation of Stat3 sequence-specific DNA binding and transcription by p300/CREB-binding protein-mediated acetylation. *J Biol Chem* **280**, 11528-34.

Waterhouse, A., Bertoni, M., Bienert, S., Studer, G., Tauriello, G., Gumienny, R., Heer, F. T., de Beer, T. A. P., Rempfer, C., Bordoli, L. et al. (2018). SWISS-MODEL: homology modelling of protein structures and complexes. *Nucleic Acids Res* **46**, W296-W303.

Weinberg, Z. Y. and Puthenveedu, M. A. (2019). Regulation of G protein-coupled receptor signaling by plasma membrane organization and endocytosis. *Traffic* **20**, 121-129.

Wenta, N., Strauss, H., Meyer, S. and Vinkemeier, U. (2008). Tyrosine phosphorylation regulates the partitioning of STAT1 between different dimer conformations. *Proc Natl Acad Sci U S A* **105**, 9238-43.

Wright, V. M., Vogt, K. L., Smythe, E. and Zeidler, M. P. (2011). Differential activities of the Drosophila JAK/STAT pathway ligands Upd, Upd2 and Upd3. *Cell Signal* **23**, 920-7.

Yan, R., Small, S., Desplan, C., Dearolf, C. R. and Darnell, J. E., Jr. (1996). Identification of a Stat gene that functions in Drosophila development. *Cell* **84**, 421-30.

Zeidler, M. P. and Bausek, N. (2013). The Drosophila JAK-STAT pathway. *JAKSTAT* **2**, e25353.

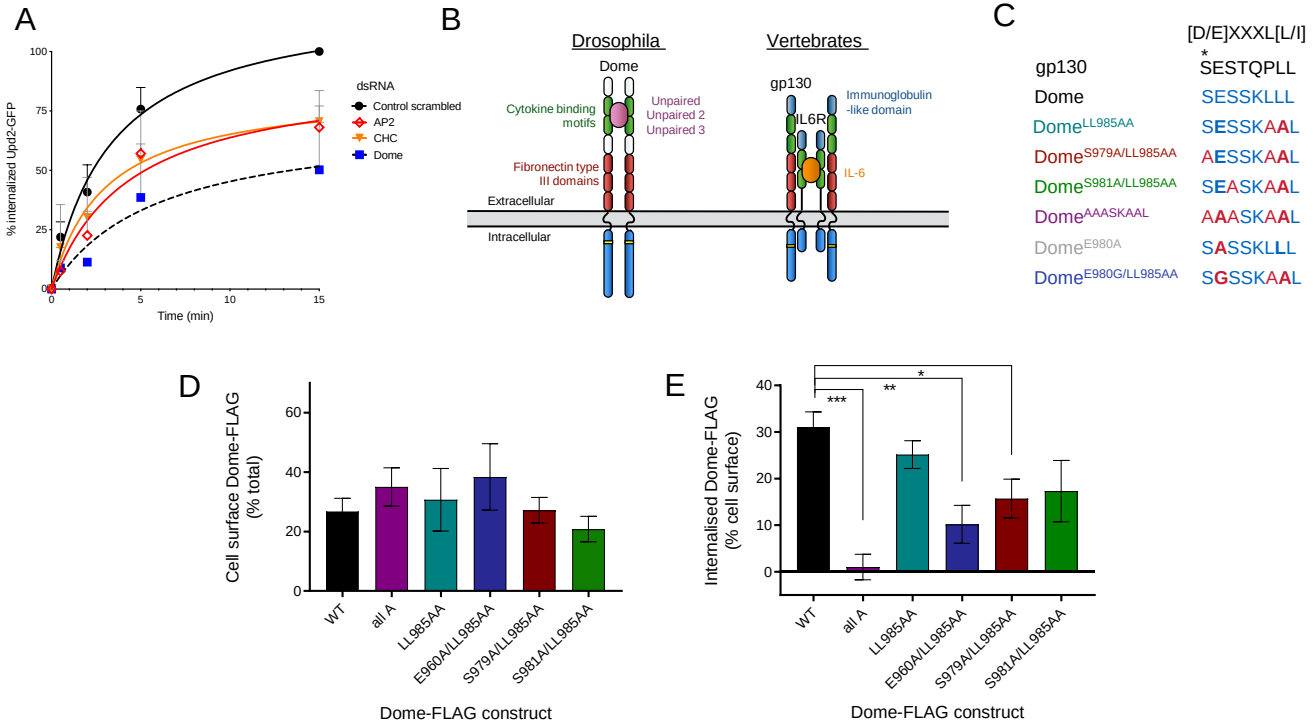
A
% internalized Upd2-GFP
Time (min)
dsRNA
Control scrambled
AP2
CHC
Dome
B
Drosophila
Vertebrates
Dome
gp130
IL6R
Cytokine binding motifs
Unpaired
Unpaired 2
Unpaired 3
Fibronectin type III domains
Immunoglobulin -like domain
IL-6
Extracellular
Intracellular
C
[D/E]XXXL[L/I]
gp130 SESTQPLL
Dome SESSKLLL
Dome^LL985AA SESSKAAL
Dome^S979A/LL985AA AESSKAAL
Dome^S981A/LL985AA SEASKAAL
Dome^AAASKAAL AAASKAAL
Dome^E980A SASSKLLL
Dome^E980G/LL985AA SGSSKAAL
D
Cell surface Dome-FLAG (% total)
WT
all A
LL985AA
E960A/LL985AA
S979A/LL985AA
S981A/LL985AA
Dome-FLAG construct
E
Internalised Dome-FLAG (% cell surface)
***
**
*
Dome-FLAG construct
F
Dome-FLAG:
WT
all A
LL985AA
E960A/LL985AA
S979A/LL985AA
S981A/LL985AA
MESNa:
Time +Upd2-GFP:
anti-FLAG
Biotin IP
Total
anti-β actin
245
190
135
46

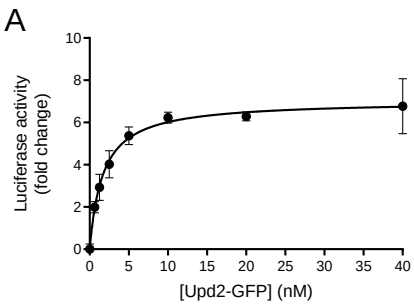
A
Luciferase activity (fold change)
[Upd2-GFP] (nM)

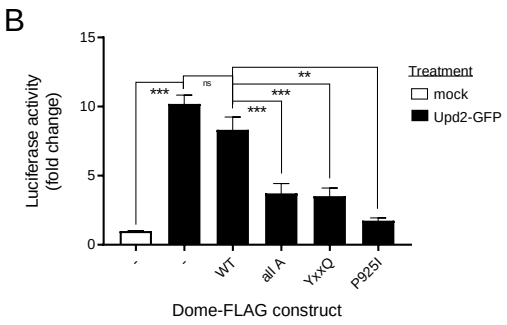
B
Luciferase activity (fold change)
Treatment
mock
Upd2-GFP
ns
WT
all A
YxxQ
P925I
Dome-FLAG construct

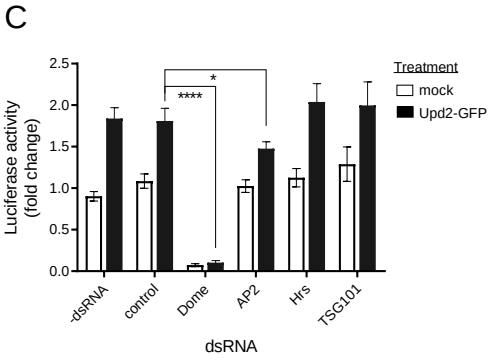
C
Luciferase activity (fold change)
Treatment
mock
Upd2-GFP
-dsRNA
control
Dome
AP2
Hrs
TSG101
dsRNA

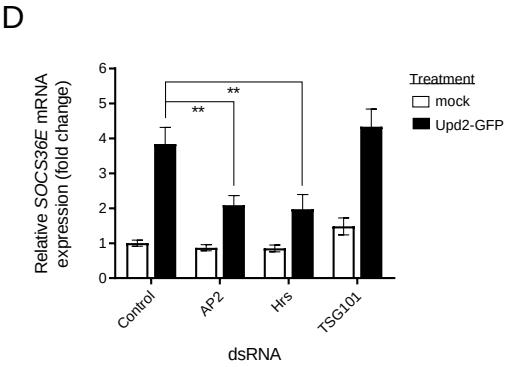
D
Relative SOCS36E mRNA expression (fold change)
Treatment
mock
Upd2-GFP
Control
AP2
Hrs
TSG101
dsRNA

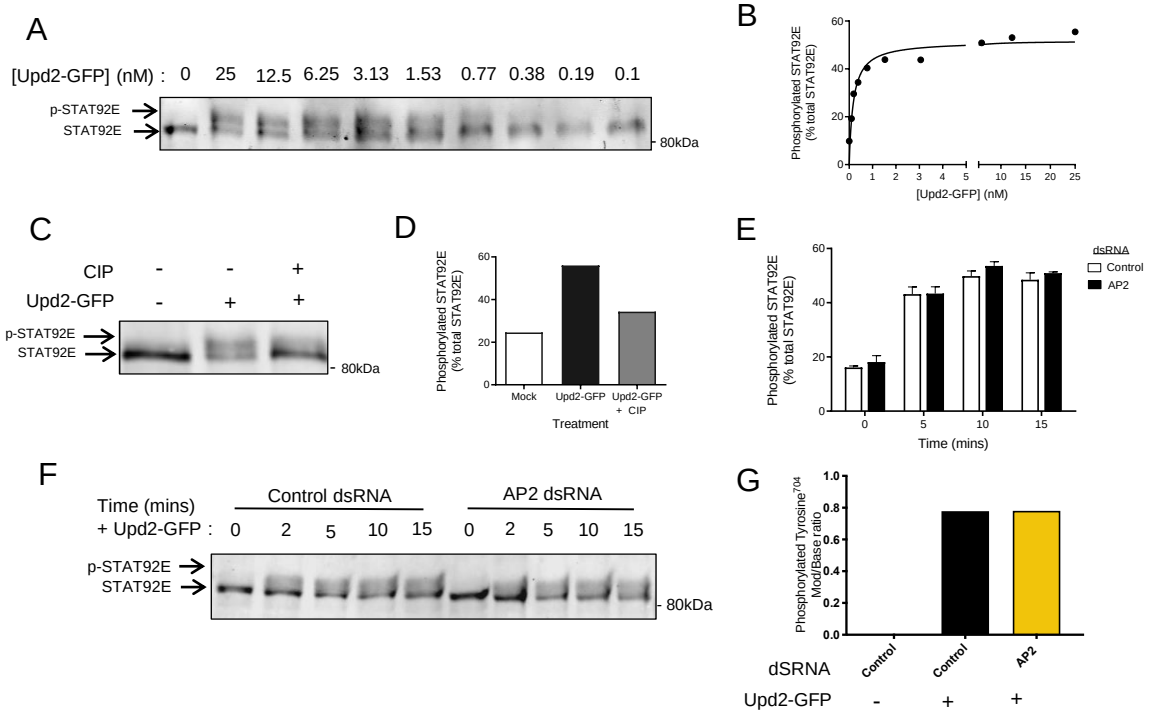
A
[Upd2-GFP] (nM) : 0 25 12.5 6.25 3.13 1.53 0.77 0.38 0.19 0.1
p-STAT92E
STAT92E
80kDa
B
Phosphorylated STAT92E (% total STAT92E)
[Upd2-GFP] (nM)
C
CIP - - +
Upd2-GFP - + +
p-STAT92E
STAT92E
80kDa
D
Phosphorylated STAT92E (% total STAT92E)
Mock
Upd2-GFP
Upd2-GFP + CIP
Treatment
E
dsRNA
Control
AP2
Phosphorylated STAT92E (% total STAT92E)
Time (mins)
F
Time (mins)
+ Upd2-GFP : 0 2 5 10 15 0 2 5 10 15
Control dsRNA
AP2 dsRNA
p-STAT92E
STAT92E
80kDa
G
Phosphorylated Tyrosine704 Mod/Base ratio
dSRNA Control Control AP2
Upd2-GFP - + +

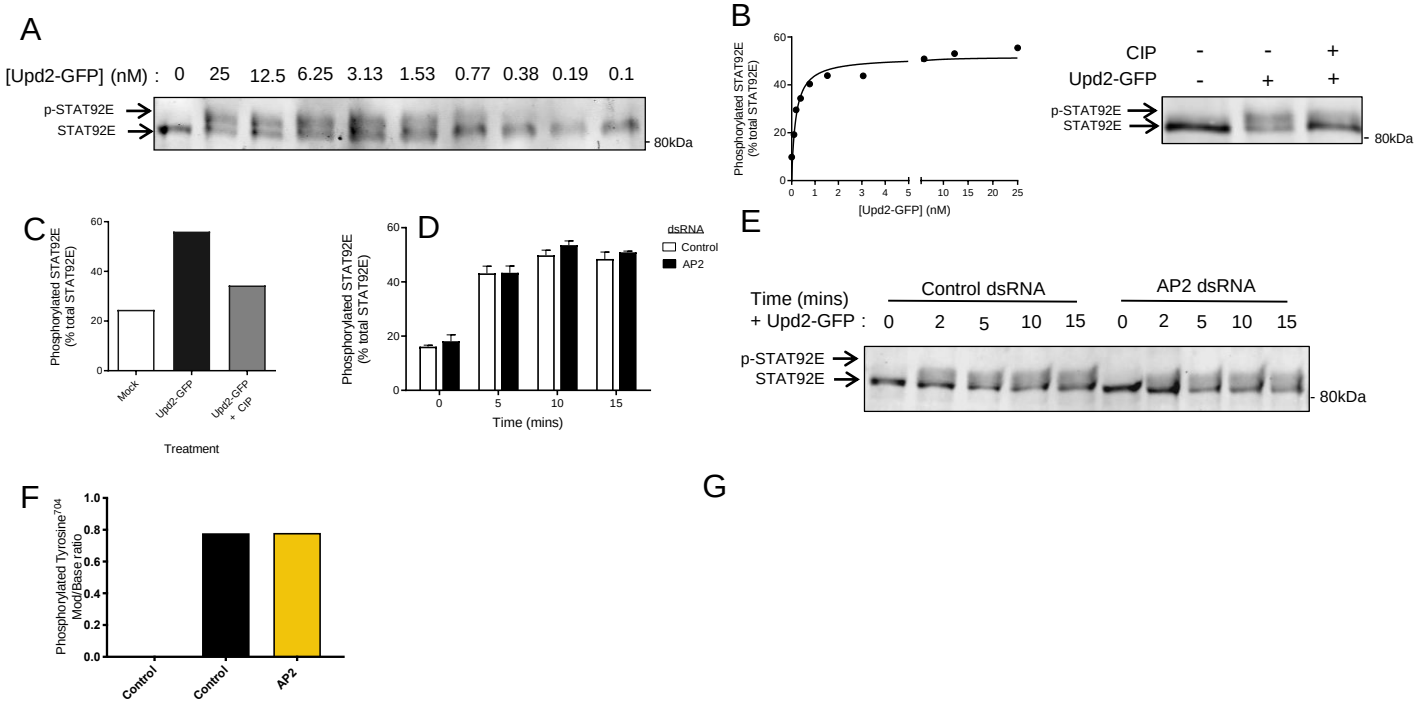
A
[Upd2-GFP] (nM) : 0 25 12.5 6.25 3.13 1.53 0.77 0.38 0.19 0.1
p-STAT92E
STAT92E
80kDa
B
Phosphorylated STAT92E (% total STAT92E)
[Upd2-GFP] (nM)
CIP - - +
Upd2-GFP - + +
p-STAT92E
STAT92E
80kDa
C
Phosphorylated STAT92E (% total STAT92E)
Mock
Upd2-GFP
Upd2-GFP + Cip
Treatment
D
Phosphorylated STAT92E (% total STAT92E)
dsRNA
Control
AP2
Time (mins)
E
Time (mins)
Control dsRNA
AP2 dsRNA
+ Upd2-GFP : 0 2 5 10 15 0 2 5 10 15
p-STAT92E
STAT92E
80kDa
F
Phosphorylated Tyrosine704 Mod/Base ratio
Control
Control
AP2
G

(f)

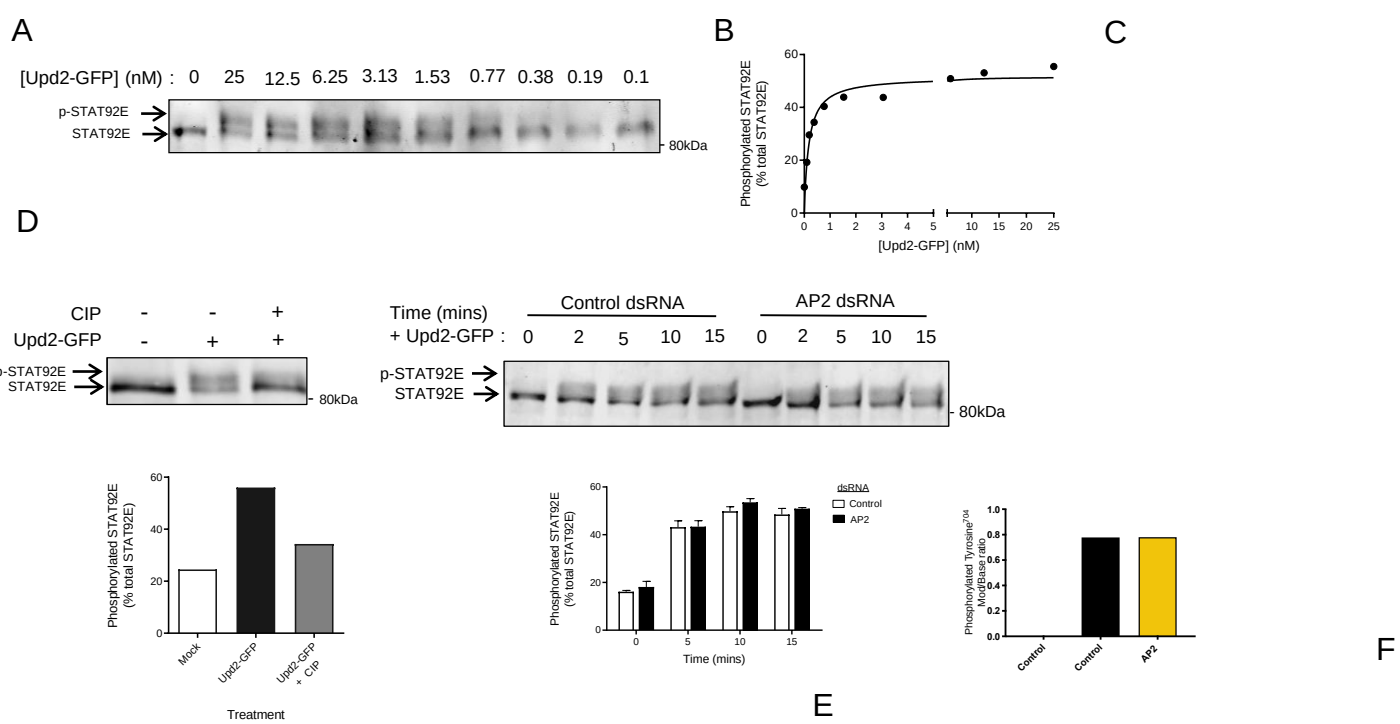
A
[Upd2-GFP] (nM) : 0 25 12.5 6.25 3.13 1.53 0.77 0.38 0.19 0.1
p-STAT92E
STAT92E
80kDa
B
Phosphorylated STAT92E (% total STAT92E)
[Upd2-GFP] (nM)
C
D
CIP - - +
Upd2-GFP - + +
p-STAT92E
STAT92E
80kDa
Time (mins)
+ Upd2-GFP : 0 2 5 10 15 0 2 5 10 15
Control dsRNA
AP2 dsRNA
p-STAT92E
STAT92E
80kDa
Phosphorylated STAT92E (% total STAT92E)
Mock
Upd2-GFP
Upd2-GFP + CIP
Treatment
E
dsRNA
Control
AP2
Phosphorylated STAT92E (% total STAT92E)
Time (mins)
Phosphorylated Tyrosine704 /totBase ratio
Control
Control
AP2
F

(f)

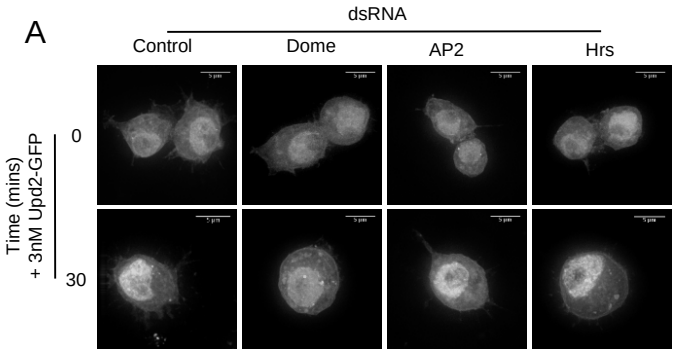
A
dsRNA
Control
Dome
AP2
Hrs
Time (mins)
+ 3nM Upd2-GFP
0
30

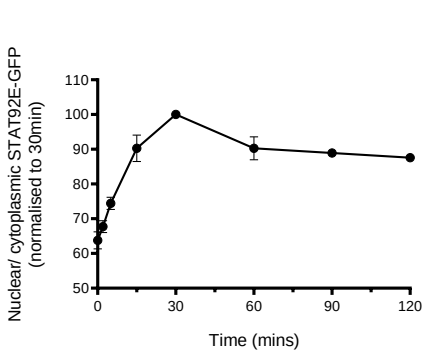
B
Nuclear/ cytoplasmic STAT92E-GFP
(normalised to 30min)
110
100
90
80
70
60
50
0
30
60
90
120
Time (mins)

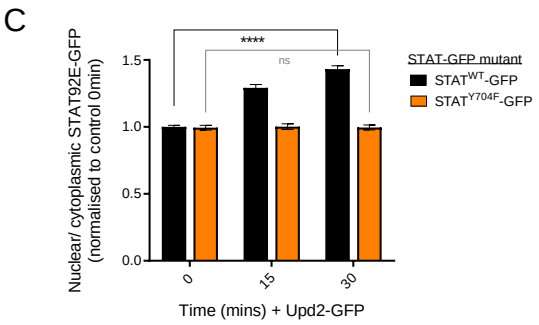
C
Nuclear/ cytoplasmic STAT92E-GFP
(normalised to control 0min)
****
ns
1.5
1.0
0.5
0.0
0
15
30
Time (mins) + Upd2-GFP
STAT-GFP mutant
STATWT-GFP
STATY704F-GFP

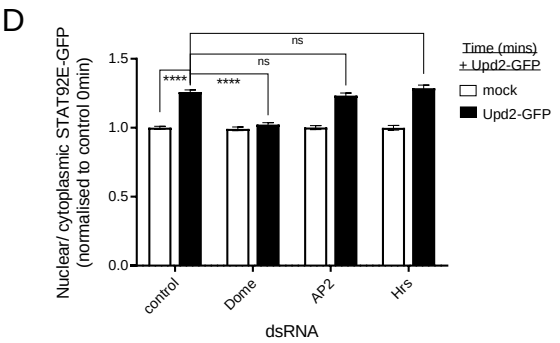
D
Nuclear/ cytoplasmic STAT92E-GFP
(normalised to control 0min)
ns
ns
****
****
1.5
1.0
0.5
0.0
control
Dome
AP2
Hrs
dsRNA
Time (mins)
± Upd2-GFP
mock
Upd2-GFP

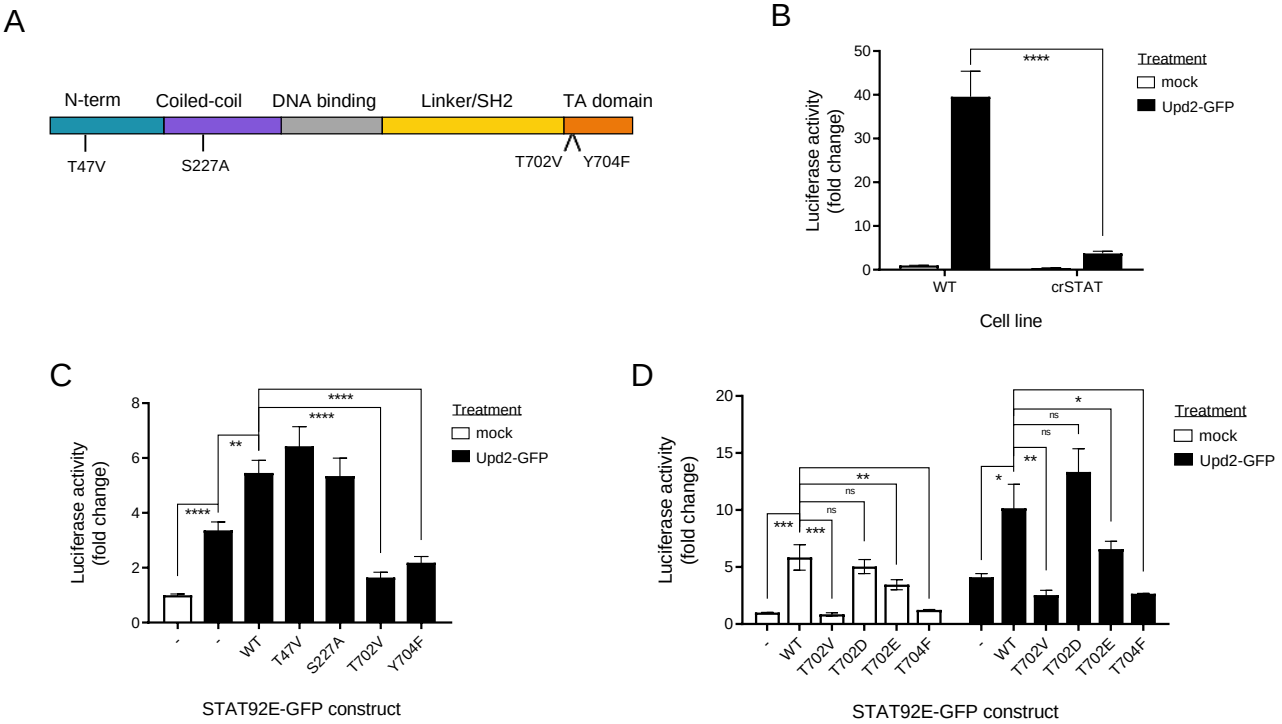
A
N-term
Coiled-coil
DNA binding
Linker/SH2
TA domain
T47V
S227A
T702V
Y704F
B
Luciferase activity (fold change)
Treatment
mock
Upd2-GFP
****
WT
crSTAT
Cell line
C
Luciferase activity (fold change)
Treatment
mock
Upd2-GFP
STAT92E-GFP construct
WT
T47V
S227A
T702V
Y704F
D
Luciferase activity (fold change)
Treatment
mock
Upd2-GFP
ns
STAT92E-GFP construct
WT
T702V
T702D
T702E
T704F

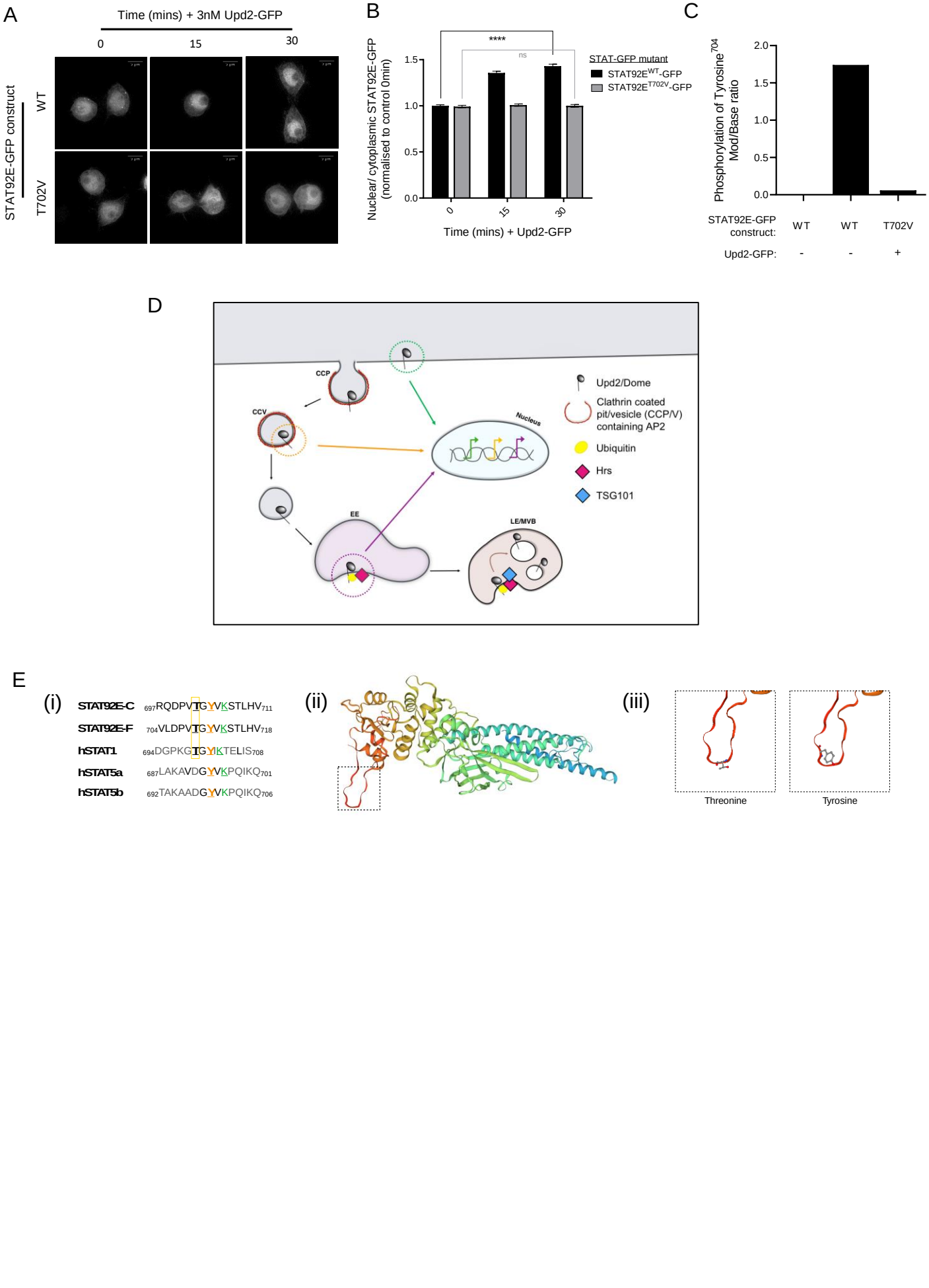
A
Time (mins) + 3nM Upd2-GFP
0
15
30
STAT92E-GFP construct
WT
T702V
B
Nuclear/ cytoplasmic STAT92E-GFP
(normalised to control 0min)
****
ns
STAT-GFP mutant
STAT92E^WT-GFP
STAT92E^T702V-GFP
Time (mins) + Upd2-GFP
C
Phosphorylation of Tyrosine^704
Mod/Base ratio
STAT92E-GFP construct:
WT
WT
T702V
Upd2-GFP:
-
-
+
D
CCP
CCV
EE
Nucleus
LE/MVB
Upd2/Dome
Clathrin coated pit/vesicle (CCP/V) containing AP2
Ubiquitin
Hrs
TSG101
E
(i)
STAT92E-C 697RQDPVTGYVKSTLHV711
STAT92E-F 704VLDPVTGYVKSTLHV718
hSTAT1 694DGPKGTGYIKTELIS708
hSTAT5a 687LAKAVDGYVKPQIKQ701
hSTAT5b 692TAKAADGYVKPQIKQ706
(ii)
(iii)
Threonine
Tyrosine